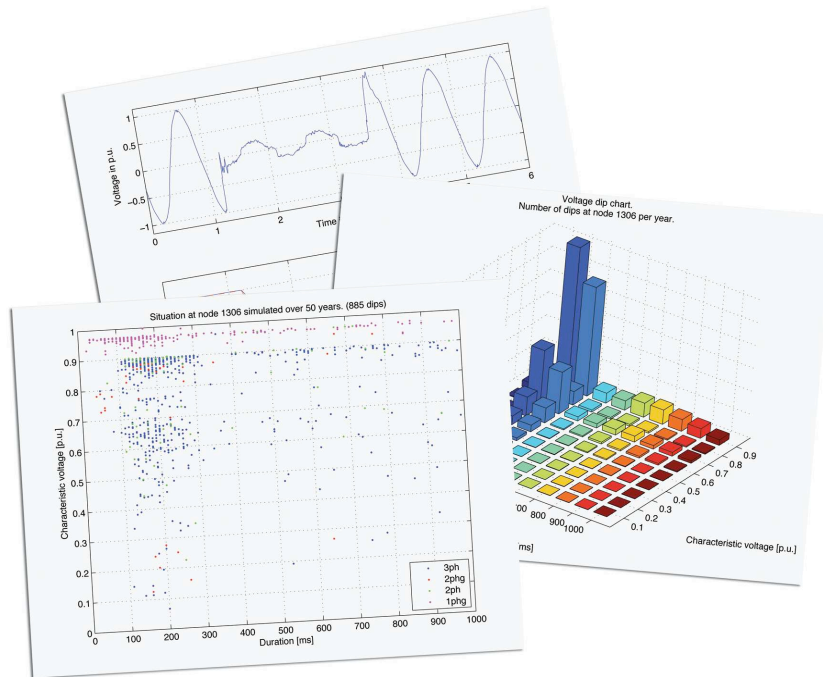


CHALMERS



Calculating voltage dips in power systems using probability distributions of dip durations and implementation of the Moving Fault Node method

Master of Science Thesis

MIKAEL WÄMUNDSON

Department of Energy and Environment
Division of electric power engineering
Masters program in Electric Power Engineering
CHALMERS UNIVERSITY OF TECHNOLOGY
Göteborg, Sweden, 2007

Calculating voltage dips in power systems

using probability distributions of dip durations
and implementation of the Moving Fault Node method

MIKAEL WÄMUNDSON

Department of Energy and Environment
Division of electric power engineering
CHALMERS UNIVERSITY OF TECHNOLOGY
Göteborg, Sweden, 2007

Calculating voltage dips in power systems
using probability distributions of dip durations
and implementation of the Moving Fault Node method

MIKAEL WÄMUNDSON

© MIKAEL WÄMUNDSON, 2007.

Department of Energy and Environment
Division of electric power engineering
Chalmers University of Technology
SE-412 96 Göteborg
Sweden
Telephone +46 (0)31-772 1000

Cover:

Pictures from back to top: example of voltage dip in one phase, a voltage dip density chart and a scatter plot.

Department of Energy and Environment
Göteborg, Sweden, 2007

Calculating voltage dips in power systems
using probability distributions of dip durations
and implementation of the Moving Fault Node method

MIKAEL WÄMUNDSON

Department of Energy and Environment
Division of electric power engineering
Chalmers University of Technology

Summary

This report is based on a master thesis work aimed at improving the Simpov Dips program, by implementing new features. Simpov Dips, in its existing version, simulates faults in all nodes in a given network and creates a result-file containing the during-fault voltages at each node for every fault. Improvements have been made in three aspects: the ability to also calculate the dip duration, an improved method for calculating the magnitude of the dip and a graphical presentation of the calculation results.

A method for defining statistical distributions of dip durations for subsets of the network has been implemented in Simpov Dips. The method is able to produce calculation results with good accuracy under an important condition: that the data used as basis for the distributions is of sufficient accuracy. This data can be collected in different ways, but monitoring the network (or a network with similar characteristics) together with knowledge of the protection relay settings can give data of desired accuracy.

In the existing version of Simpov Dips the dip magnitudes are calculated with faults only occurring at the nodes. The Moving Fault Node method implemented in the new version of Simpov Dips will result in more accurate calculations of the magnitude.

The calculation according to this method requires the bus impedance matrix, the impedance for the faulted line, the fault position on the line and pre-fault voltages at three locations in the system: the two terminals of the faulted line and the node where the customer is connected. A uniform distribution of the fault position over the line length has been assumed.

The calculation of the dip magnitude for a fault at a line is not yet implemented in Simpov Dips itself, but is done in an analysis program, written under Matlab. The result-file produced by Simpov Dips gives pre-fault voltages and sequence impedances necessary for the calculation.

The above-mentioned analysis program also produces graphical presentations of the results: scatter plots, voltage dip coordination charts and voltage dip density charts are produced. The voltage dip coordination chart is helpful when estimating the severity of the dip situation for a certain customer by introducing the voltage-tolerance curve. By using the voltage dip density chart and cumulative chart an impression of the power quality is given for the site.

The different plots also simplify the analysis of the effect of changes in the power system. This is illustrated for a number of different changes to a small network.

Keywords: voltage dip, duration, statistical distribution, power system, power quality, moving fault node method

Acknowledgements

This work has been carried out at STRI AB, and I would like to thank my supervisor Math Bollen for showing such a big interest in my efforts. Also, Magnus Speychal at STRI has been very helpful, thank you! The project has been supported by Vattenfall in Trollhättan, and I would like to thank Per Norberg for his help—and the guided tour—and also Thomas Gustafsson for his inputs on fault-clearing times. Finally, I would like to thank my examiner at Chalmers, Torbjörn Thiringer.

Mikael Wämundson
Göteborg, 2007

Contents

1	Introduction	1
2	Dips — classification, magnitude and duration	3
2.1	Classification of unbalanced dips	5
2.2	Calculation of the balanced dip magnitude	7
2.3	Calculation of the characteristic magnitude	7
2.4	Voltage dip duration	9
2.5	Other characteristics of the dip	12
2.6	Voltage dip impacts on equipment	13
2.7	Economic costs due to voltage dips	15
3	Existing software	17
4	Improvements in the software	19
4.1	Calculation of dip duration	19
4.2	Improved calculation of dip magnitude	27
4.3	Graphical representation of the result-file	31
5	Applying the improved software to a realistic network	37
5.1	Fault-frequencies	37
5.2	Dip duration distributions	39
5.3	Calculation using dip duration distributions from Table 5.2	39
5.4	Calculation using dip duration distributions from Table 5.3	45
6	Discussion	49
6.1	Calculation of dip duration	49
6.2	Calculation of dip magnitude	49
6.3	Graphical presentation of calculation results	50
7	Future work	51
A	Simpow files used in calculation	55
A.1	Optpow file	55
A.2	Dynpow file	57
A.3	Fault-information file	58

1 Introduction

In recent years greater concern has been given within power quality to a phenomenon called voltage dips or sags. A voltage dip is a temporary decrease in voltage magnitude. The economic losses in the industry due to these voltage dips are significant, and both customers and network operators have an interest in minimizing the number of dips and their consequences. A method described in this report to get a comprehension of the voltage dip situation—at a customer connection or a part of a power network—is computer calculations based on both network parameters and stochastic variables. The report focuses on two main attributes of the voltage dip: the magnitude and duration.

The report is based on a master thesis work aimed at improving an existing calculation software, Simpov Dips, by implementing new features. Simpov Dips, in its existing version, simulates faults in all nodes in a given network and creates a result-file containing the during-fault voltages at each node for every fault. Improvements have been made in three aspects: the ability to also calculate the dip duration, an improved method for calculating the magnitude of the dip and a graphical presentation of the calculation results.

A theoretical background to voltage dips and why they occur in a power system is given in Chapter 2. Examples are also given here on how to calculate the magnitude of the dip. An important attribute of the voltage dip is its duration, and the factors affecting the dip duration are discussed in a subsection. Also, the effect of voltage dips on equipment connected to the grid, and the resulting economic consequences, are discussed in this chapter.

In Chapter 3 a detailed agenda for the improvements in the software is given and in Chapter 4 the methods used are presented. This chapter is divided in three parts: the first handles the calculation of dip duration using a statistical distribution. The second part presents how the calculation of the dip magnitude can be made more accurate by implementing a calculation method called Moving Fault Node. The third part focuses on how the calculation results are presented graphically.

Chapter 5 shows calculation results for a realistic, small network and how the effect of changes in the network can be calculated.

In Chapter 6 the methods and results of the master thesis work are discussed and some suggestions on future work are given in Chapter 7.

2 Dips — classification, magnitude and duration

Power quality problems may be of different nature, including interruptions, harmonic distortion, over- and undervoltage, flicker and voltage dips. (In many publications the term *sag* is used. This is synonymous to *dip*.) The dip—the one quality problem in focus for this report—is a result of a huge current typically flowing in some other part of the system. The current can be due to a short circuit, a starting machine or energizing of a transformer. An example of a voltage dip in one phase is plotted in Figure 2.1. The upper plot shows the voltage as function of time and the lower plot shows the calculated rms-value (with one-cycle window as solid line and half-cycle window as dashed line). The data for the dip is taken from [1]. An event of this kind can cause problems to users of electronic, and other, equipment connected to the grid. The degree of effect the dip has on the equipment depends on the severity of the dip, but also on the possibility of the equipment to withstand the dip.

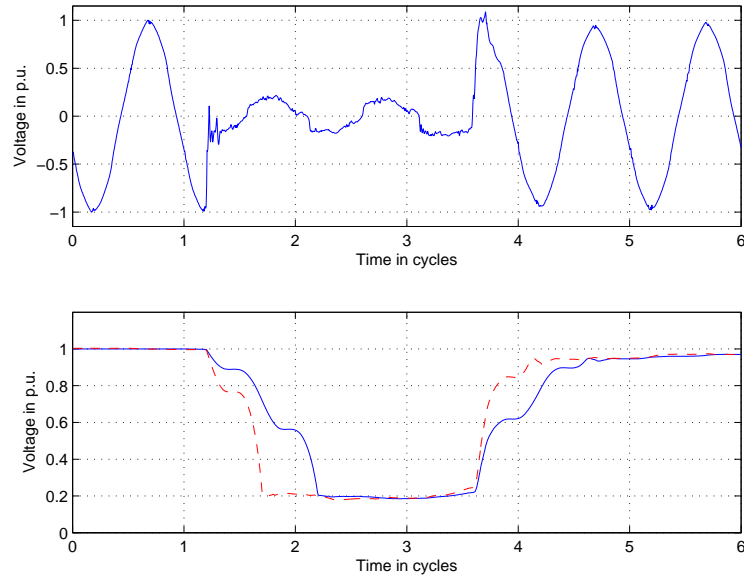


Figure 2.1: Example of voltage dip and calculated rms-value.

In IEEE Std. 1159-1995 the different power quality events are defined and this is outlined in Figure 2.2 with focus on voltage dips.

The event is classified as a dip if the voltage magnitude drops to between 10 and 90 percent of nominal voltage during 0.5 cycles up to 1 minute. Events shorter than 0.5 cycles in duration

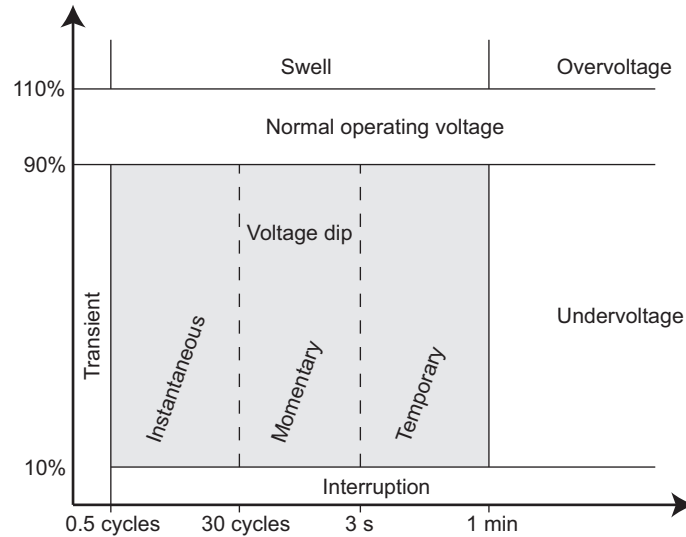


Figure 2.2: Definition of voltage dips according to IEEE Std. 1159-1995. [2]

are defined as *transients* and magnitudes lower than 10 percent of nominal value are defined as *interruptions*. If the lower magnitude is maintained for longer than 1 minute the problem is classified as an *undervoltage*. Note that in IEC documents and in many more recent publications, the term *residual voltage* is used as synonym for *magnitude*.

The voltage dip region is divided further depending on the dip duration. Between 0.5 and 30 cycles (10 to 600 ms in 50 Hz system) the dip is classified as *instantaneous*, between 30 cycles and 3 seconds it is classified as *momentary* and between 3 seconds and 1 minute the dip is defined as *temporary*. It is a natural conclusion that dips with longer duration cause bigger problems. However, this report focuses on dips due to faults with durations decided by fault-clearing times, thus durations between 0.5 cycles to 1 second are considered. Severe dips with a duration exceeding several seconds are rare and typically point to severe problems in the network.

The dip magnitude is an rms-value measured over a half or complete cycle. Some difficulties in defining the magnitude of the dip arise when there is imbalance between the phases. Faults are categorized into three-phase, two-phase, two-phase-to-ground and single-phase faults. Only three-phase faults result in a balanced voltage. For the other types of faults the voltage is unbalanced with different values in each phase. Often the phase containing the lowest voltage is chosen as reference for the magnitude and the phase containing the most prolonged dip as reference for the duration. This approach can cause problems. For example, a three-phase load experiencing a very deep single-phase dip may handle it without problem, but if the same load is exposed to a relatively shallow three-phase dip it could lead to malfunction.

A more appropriate approach is to calculate the *characteristic magnitude* as proposed in [3]. In this method the dip magnitude is derived from voltages using the method of symmetrical components. For a balanced dip (due to a three-phase fault) the characteristic magnitude is equal to the measured rms voltage but for unbalanced dips the method will take into account the degree of unbalance when calculating the magnitude. The following section covers this method of classification of dips.

2.1 Classification of unbalanced dips

In Figure 2.3 an example of a three-phase unbalanced dip is plotted. The data for the plot is taken from [1].

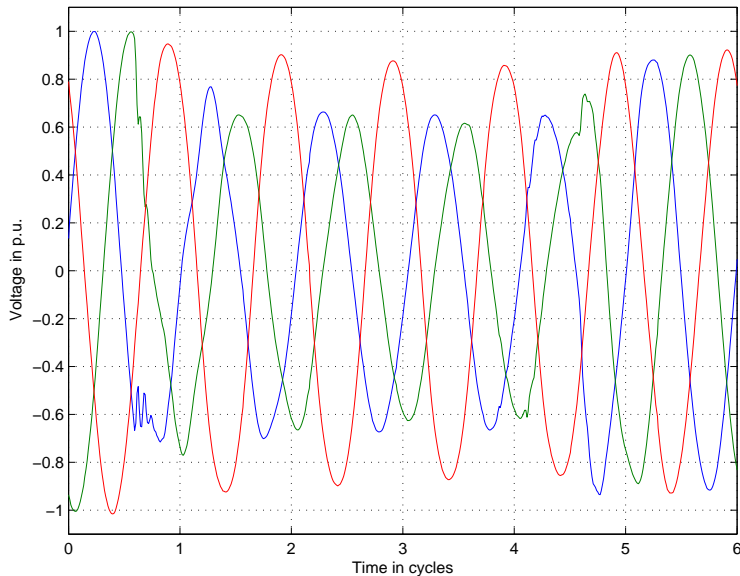


Figure 2.3: Example of a three-phase unbalanced dip. [1]

Voltage dips can mainly be classified as type A, B, C or D with pre-fault (dotted) and during-fault (solid) voltages as shown in Figure 2.4, where the three-phase voltages are represented by their phasors. A three-phase fault will result in a dip of type A for both star- and delta-connected loads. This is the only dip type with the same dip magnitude in all three phases. A single-phase fault would cause a type B dip for star-connected loads and a type C dip for delta-connected loads. A phase-to-phase fault will cause a type C dip for star-connected loads and type D dip for delta-connected loads.

A dip experienced by a certain customer can often be the result of a fault at a different voltage level and thus at least one transformer is between the customer and fault. The dip type will in most cases not be the same on the transformers high- and low-voltage sides. In Table 2.1 the dip type on the secondary side due to a dip on the primary side of the transformer is described. Upper-case letter in transformer connection corresponds to the primary side and lower-case letter to the secondary side of the transformer. Letter N stands for grounded neutral, z for zig-zag connection.

Table 2.1: Transformation of dip types A, B, C and D through transformer. [4]

Transformer connection	Type A	Type B	Type C	Type D
YNyn	Type A	Type B	Type C	Type D
Yy, Dd, Dz	Type A	Type D	Type C	Type D
Yd, Dy, Yz	Type A	Type C	Type D	Type C

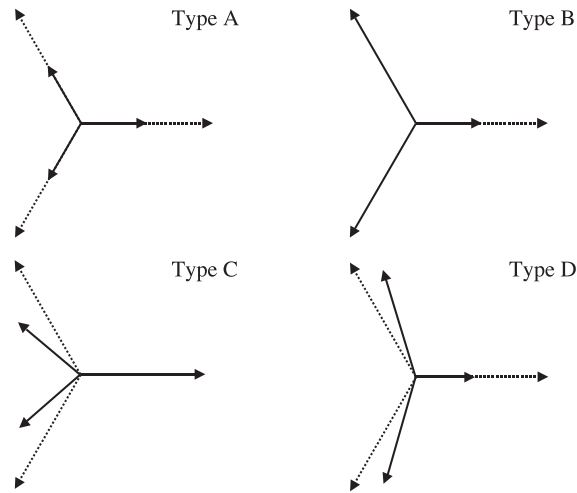


Figure 2.4: The different main types of voltage dips. [4]

Also taking into account two-phase-to-ground faults three more dip types arise: E, F and G as shown in Figure 2.5.

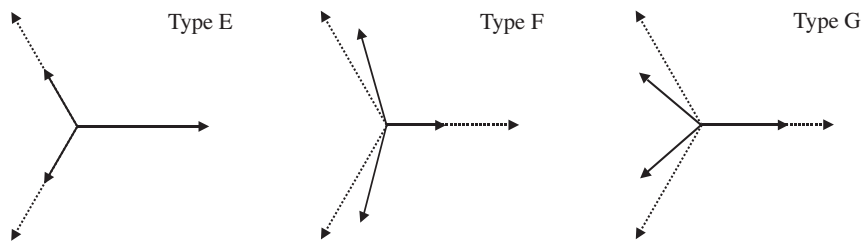


Figure 2.5: Dip types due to two-phase-to-ground faults. [4]

These dip types can not be transformed from or to the previously mentioned dip types (A, B, C and D) but transformation between the types E, F and G is possible as shown in Table 2.2.

Table 2.2: Transformation of dip types E, F and G through transformer. [4]

Transformer connection	Type E	Type F	Type G
YNyn	Type E	Type F	Type G
Yy, Dd, Dz	Type G	Type F	Type G
Yd, Dy, Yz	Type F	Type G	Type F

In addition to the dip type uppercase letter, A to G, a lowercase letter is used to describe in which phase (or phases) the main voltage drop occurs. Thus, a dip of type Ba corresponds to single-phase-to-ground fault in phase *a*, a dip of type Ca corresponds to a phase-to-phase fault between phases *b* and *c* (the main voltage drop occurs in phases *b* and *c*). Using this method the necessary information about the dip is represented in just two letters.

To calculate the characteristic magnitude knowledge of the three-phase voltages or sequence voltages is required. Before this calculation method is explained the more simple case with a balanced dip is examined.

2.2 Calculation of the balanced dip magnitude

The dip magnitude during a fault is dependent on two impedances, the source impedance, Z_S , and the impedance to the fault, Z_F (a third impedance, the actual impedance between fault point and ground is often ignored). With a simple model using voltage division the dip magnitude at a certain node in the system can be calculated. This is shown in Figure 2.6. This model holds only if the system is radial, i.e. the bus is only fed from source in the figure. In case of more complicated meshed systems, calculation methods making use of node impedance/admittance matrices are applied to the problem.

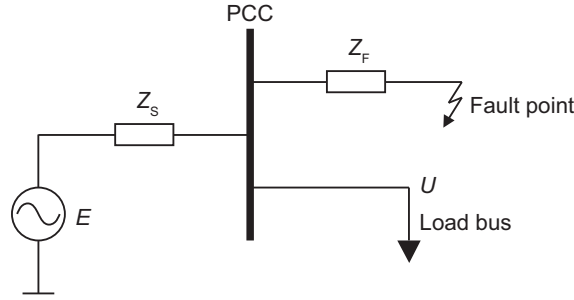


Figure 2.6: Model to calculate balanced dip magnitude.

EXAMPLE 2.1 Consider the system in Figure 2.6 with $E = 1$, $Z_S = 0.5$ and $Z_F = 2$ (all values in p.u.). The during-fault voltage, U , at the load bus due to a three-phase fault at the fault point would be

$$U = E \frac{Z_F}{Z_S + Z_F} = 1 \frac{2}{0.5 + 2} = 0.8 \text{ p.u.} \quad (2.1)$$

■

EXAMPLE 2.2 Use the same values as for the previous example but put $Z_S = 2$ to represent a weaker grid. The during-fault voltage would now be

$$U = E \frac{Z_F}{Z_S + Z_F} = 1 \frac{2}{2 + 2} = 0.5 \text{ p.u.} \quad (2.2)$$

■

From these two examples we can draw the simple conclusion that a strong grid will prevent deep voltage dips.

2.3 Calculation of the characteristic magnitude

Unbalanced situations in power systems are successfully treated using symmetrical components, a method described in most textbooks on power systems. The three-phase voltages (U_a , U_b , U_c) are transformed to positive, negative and zero sequence voltages (U_1 , U_2 , U_0) using the the transformation matrix \mathbf{A} . With

$$\mathbf{A} = \begin{bmatrix} 1 & 1 & 1 \\ \alpha^2 & \alpha & 1 \\ \alpha & \alpha^2 & 1 \end{bmatrix}, \quad \mathbf{U}_{\text{phase}} = \begin{bmatrix} U_a \\ U_b \\ U_c \end{bmatrix} \quad \text{and} \quad \mathbf{U}_{\text{sequence}} = \begin{bmatrix} U_1 \\ U_2 \\ U_0 \end{bmatrix}$$

we have

$$\mathbf{U}_{\text{phase}} = \mathbf{A}\mathbf{U}_{\text{sequence}} \quad \text{or} \quad \mathbf{U}_{\text{sequence}} = \mathbf{A}^{-1}\mathbf{U}_{\text{phase}}.$$

Here α is defined as a rotation of 120 degrees in the complex plane, i.e.

$$\alpha = -\frac{1}{2} + j\frac{1}{2}\sqrt{3}. \quad (2.3)$$

Each power system has its specific sequence impedances and from the model in Figure 2.7 the sequence voltages at the load bus can be calculated. Observe that for each type of fault the individual model of the system changes. For a detailed description of this, see [4]. The positive and negative sequence voltages, U_1 and U_2 , at the load bus can now be calculated. The two voltages are complex with magnitude and phase.

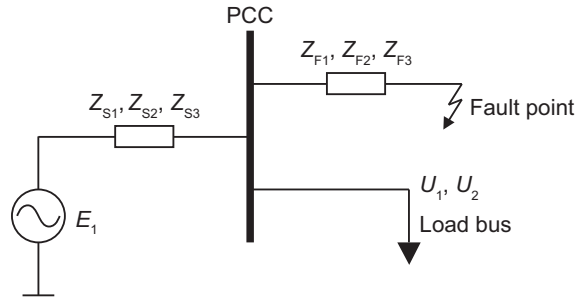


Figure 2.7: Model to calculate unbalanced dip magnitude.

EXAMPLE 2.3 For a phase-to-phase fault U_1 and U_2 would have the following values

$$U_1 = E_1 \left(1 - \frac{Z_{S1}}{Z_{S1} + Z_{S2} + Z_{F1} + Z_{F2}} \right) \quad (2.4)$$

$$U_2 = E_1 \frac{Z_{S2}}{Z_{S1} + Z_{S2} + Z_{F1} + Z_{F2}} \quad (2.5)$$

■

Two properties of the unbalanced dip can be calculated from the positive and negative sequence voltages, U_1 and U_2 : the *characteristic voltage* and *PN factor*. The definitions of these properties for different dip types are presented in Table 2.3. As before, α is defined as a rotation of 120 degrees in the complex plane.

EXAMPLE 2.4 Continuing Example 2.3, assume we have dip of type Ca. The characteristic voltage is then

$$U_1 - U_2 = E_1 \frac{Z_{F1} + Z_{F2}}{Z_{S1} + Z_{S2} + Z_{F1} + Z_{F2}} \quad (2.6)$$

and the PN factor

$$U_1 + U_2 = E_1 \left(1 - \frac{Z_{S1} - Z_{S2}}{Z_{S1} + Z_{S2} + Z_{F1} + Z_{F2}} \right) \quad (2.7)$$

■

Table 2.3: Definitions of characteristics for three-phase unbalanced dips. [5]

Dip type	Drop in phases	Characteristic voltage	PN factor
Ca	bc	$U_1 - U_2$	$U_1 + U_2$
Cb	ac	$U_1 - \alpha^2 U_2$	$U_1 + \alpha^2 U_2$
Cc	ab	$U_1 - \alpha U_2$	$U_1 + \alpha U_2$
Da	a	$U_1 + U_2$	$U_1 - U_2$
Db	b	$U_1 + \alpha^2 U_2$	$U_1 - \alpha^2 U_2$
Dc	c	$U_1 + \alpha U_2$	$U_1 - \alpha U_2$

The *characteristic magnitude* is now defined as the absolute value of the characteristic voltage. For a dip of type Ca, as in Example 2.4, it would be $|U_1 - U_2|$. The characteristic magnitude can be used for unbalanced dips in the same way as the magnitude for balanced dips that was covered in Section 2.2. The dip type can be determined from the fault type and transformer winding connections or from the angle between positive and negative sequence voltages.

Some conclusions for this method are drawn in [5]. For dips due to three-phase, two-phase-to-ground and phase-to-phase faults the characteristic magnitude values are the same for faults at the same location, but for single-phase faults the characteristic magnitude is strongly dependent on the system grounding. With high-impedance grounding the characteristic magnitude for a dip due to a single-phase fault will be close to 1 p.u., i.e. a very shallow dip.

2.4 Voltage dip duration

A main topic for this report is the voltage dip duration. Together with the magnitude the duration forms the two most important attributes of the voltage dip. As seen in the previous section, dip magnitude, and also the characteristic magnitude, are controlled by the impedances in the power system. The dip duration, however, is the result of settings in protection relays throughout the system, or start-up times for large machines. In this report we focus on dips as a result of faults in the system and thus we are interested in how different protection systems affect the fault-clearing time and thereby the dip duration. In this section we look at the methods of protection throughout the different areas of a electric network.

The fault-clearing time of a protection relay can be divided into two different parts: the *relay operating time* (including some intentional time delay needed for protection coordination) and the *circuit breaker interrupting time*. The relay operating time is the time interval from the instant the fault is detected (using different methods) until a tripping signal is sent to the circuit breaker. The circuit breaker interrupting time is the time it takes for the circuit breaker to completely interrupt the current.

In high voltage transmission systems, faults lead to very large currents that of course can cause severe damage, but there is also an even more serious effect. If the dip duration is too long it causes instability in the system, which in turn may lead to very large black-outs. Therefore a fast response of the protection system and short fault-clearing time is critical. The protection systems used are distance and differential protection with fault-clearing times ranging from 50 to 300 ms (2.5 to 15 cycles). At the lower voltage levels used in radial networks for distribution the method of protection is mainly overcurrent relays with time delay. The fault-clearing time is ranging from 200 to 2000 ms (10 to 100 cycles). At the lowest voltage levels with less need for redundancy fuses are used. When blown, these can not be automatically replaced

and cause longer interruptions. Fault-clearing times are ranging from 10 to 1000 ms (0.5 to 50 cycles). Generators, busbars and transformers are protected using differential relays with fault-clearing times between 100 and 300 ms (5 to 15 cycles). Here follows a description of the different protection systems.

2.4.1 Distance protection (50–100 ms)

Consider the system in Figure 2.8, which is part of a larger meshed system with power that can be fed from different sources to busses 1, 3 and 4. If a fault occurs at point a there will be a large increase in the current through the breaker B_{12} . Also the voltage at bus 1 will drop in magnitude. By sensing the ratio V_1/I_{12} we will have a very sensitive method of detecting the fault. The value V_1/I_{12} can be seen as the impedance λZ_{12} , where λ is the fraction of the line length between bus 1 and 2 and Z_{12} is the total line impedance. Assume that the protection system is set to trip the breaker B_{12} if the ratio $|V_1/I_{12}| = \lambda|Z_{12}| < Z_C$. This expression can then be seen as this: for a fault up to a certain distance from bus 1 the breaker will trip. This kind of protection is therefore called both impedance and distance protection. The method is well suited for meshed transmission networks.

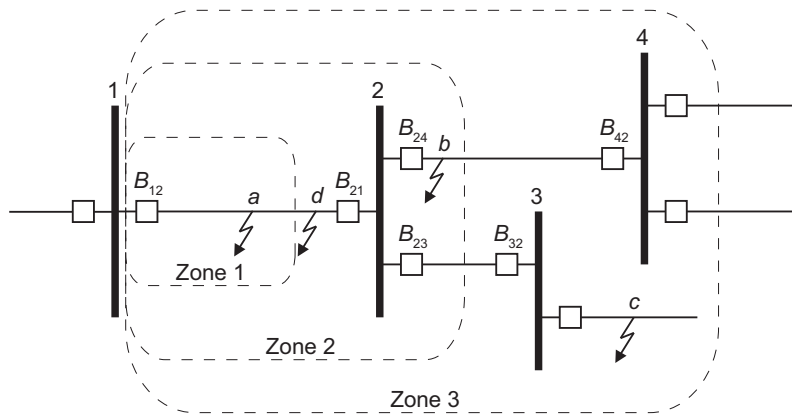


Figure 2.8: Protection using distance relays.

By using several distance relays for each breaker different zones of protection are possible. For zone 1 (see figure!) Z_C is set to about 80% of the line length and the relay is configured to activate the breaker as quickly as possible. For zone 2 the relay is configured with a Z_C that reaches past the next bus (point b in figure) and is set to activate the breaker after a certain time delay (around 500 ms). After another time delay the relay for zone 3 is tripping the breaker for faults even further away (point c in figure). In normal operation of the system only zone 1 protection is activated. A fault at point b is of course in zone 1 of breaker B_{24} protection system, and a fault at point c is in zone 1 of the protection system at bus 3. We would of course want zone 2 and 3 protection relays to only be activated when zone 1 protection is not clearing the fault due to some error. But what if a fault occurs at point d ? The protection relay for zone 1 only covers around 80% of the line length and obviously does not trip the breaker for 20% of the faults on the line (if the fault frequency is evenly distributed over the length of the line). The fault in point d therefore activates the protection relay for zone 2 and the fault-clearing time is prolonged significantly compared to if the fault had been cleared in zone 1. This is an unavoidable consequence of the protection system.

Also consider the possibility of a malfunctioning breaker, i.e. the protection relay has picked up the fault and sent a tripping signal to the breaker, which in turn does not operate to clear the

fault. Since the fault is not cleared the protection relay of the next zone will react and a larger part of the system than necessary will be affected. The malfunctioning breaker can be discovered using breaker-failure protection. This is implemented by using a second protection relay, which is also sensing the current through the controlled breaker. If the breaker is malfunctioning this second relay discovers that the current through the breaker still flows and reacts to this. How? As an example, consider breaker B_{24} in Figure 2.8. Assume that there is a fault at point b and this breaker is malfunctioning. Without breaker-failure protection this would cause breaker B_{12} to be tripped by its zone 2 protection relay. With breaker-failure protection the second protection relay can trip breakers B_{21} and B_{23} resulting in less affected customers. If bus 2 also can be split in two by an additional breaker, as is normally the case in transmission systems, there is a possibility that bus 3 can still be fed from bus 1.

2.4.2 Differential protection (100–300 ms)

Busbars, transformers and generators/motors are protected using differential relays. The idea of the method is to compare the current going into the protected component with the current coming out from it. If the two currents differ more than a predefined value the relay will trip a breaker. The function of a differential relay is shown in Figure 2.9.

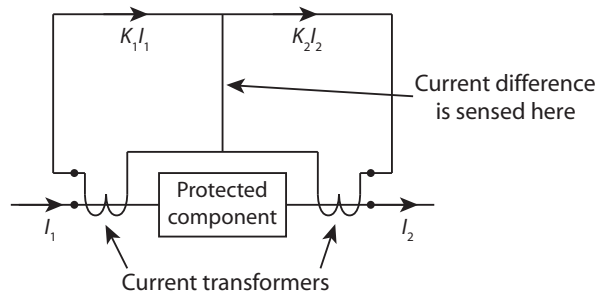


Figure 2.9: Function of a differential relay.

2.4.3 Overcurrent protection (200–2000 ms)

In radial systems in distribution networks protection is done mainly using overcurrent relays with time delay. Consider the radial system shown in Figure 2.10. The short-circuit current for a fault at point a will be higher than for a fault at point b . The overcurrent protection relay at B_2 will be set to immediately trip for a current about 1.5 times the nominal current rating of S_3 . The protection relay at B_1 is then coordinated so that it will trip immediately for a current 1.5 times the nominal current rating of S_2 plus S_3 , but with a time delay for fault currents lower than this. This coordination ensures that the overcurrent relay closest to the fault will trip first. For a fault at point b , B_2 will trip immediately, and in case of malfunction of B_2 , B_1 will trip after some delay. For a fault at point a the fault current will be large enough to immediately trip B_1 . For a long radial feeder with many overcurrent relay the coordination can lead to fault-clearing times of up to 2000 ms.

2.4.4 Fuses (10–1000 ms)

When fast reclosure after fault is not necessary a cheap protection is the use of fuses. In Figure 2.11 the use of fuses at a low voltage level is shown. The main feeders connected to the bus are protected with overcurrent relays with the possibility to reclose the breaker. The laterals

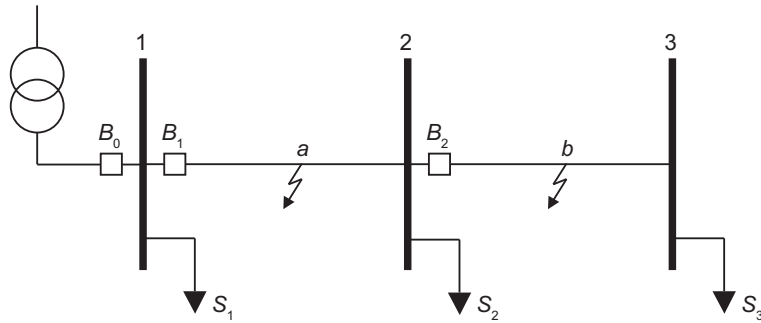


Figure 2.10: Overcurrent protection in radial systems.

connected to the feeders are protected with fuses. Time coordination between the overcurrent relays and the fuses can be introduced to prevent fuses to mitigate temporary faults, a method called fuse saving. When a fuse is blown it will need manual replacement leading to a long interruption for customers connected to the affected lateral. Other customers connected to the same feeder and busbar will experience a voltage dip with a duration related to the fuse's fault-clearing time, 10–1000 ms.

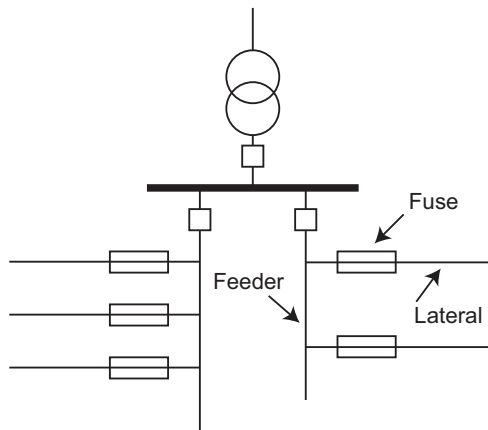


Figure 2.11: Protection of laterals using fuses.

As seen from the sections above the fault-clearing time, and as a result the dip duration, can vary considerably in the system depending on where the fault occurs. In Table 2.4 is shown fault-clearing times at different voltage levels for a U.S. utility. Observe that the fault-clearing times are distributed between a best and a worst case value around a typical, expected value. As covered in the section on distance protection the faults are cleared in different protection zones. The table only covers the first zone.

2.5 Other characteristics of the dip

During the fault there is phase displacement of the voltage compared to the voltage before and after the fault. This *phase jump* is dependent on the relation between the source and fault impedance. The phase jump is smallest for transmission systems, a bit larger for overhead line distribution systems and largest for underground cables in distribution systems. This difference can be explained by the different X/R ratios at different parts in the system.

Table 2.4: Fault-clearing times at different voltage levels. [6]

Voltage level	Best case	Typical	Worst case
525 kV	33 ms	50 ms	83 ms
345 kV	50 ms	67 ms	100 ms
230 kV	50 ms	83 ms	133 ms
115 kV	83 ms	83 ms	167 ms
69 kV	50 ms	83 ms	167 ms
34.5 kV	100 ms	2 s	3 s
12.47 kV	100 ms	2 s	3 s

The magnitude and phase jump can be calculated using the impedances of the system. However, this is not the case for the third attribute and main topic for this report, the dip duration. The duration is depending on the fault-clearing time at a fault or the acceleration of the machine causing the dip. Since dips mainly are the result of a fault (short circuit) the dip remains as long as the fault does. This is the fault-clearing time, consisting of the protection system's time to discover and react to the fault and the operation time for the circuit breaker. The fault-clearing time, and thus the dip duration, is ranging from tens of ms to some seconds. The reason for this span is the different types of protection systems used in different parts of the grid.

Except the magnitude, duration and phase jump the voltage dip also has a fourth attribute, the *point on wave*. The point on wave is not determined by the network characteristics but rather the actual moment during the cycle the fault occurs and the voltage drops. This attribute of the dip is rarely considered but can have effect on power electronic devices and on motor contactors.

2.6 Voltage dip impacts on equipment

This section will focus on the problems caused by voltage dips on electric equipment. In the previous section the four different characteristics of the voltage dip were mentioned: magnitude, duration, phase angle jump and point on wave. Different equipment can be sensitive to different dip characteristics. The most sensitive categories of equipment are considered to be computers and other electronics which are mainly powered by single-phase diode rectifiers, adjustable speed ac drives fed by three-phase rectifiers/inverters and adjustable speed dc drives fed by three-phase controlled rectifiers. Apart from these three categories contactors can be mentioned as sensitive to voltage dips.

To characterize a customer's immunity to voltage dips a voltage-tolerance curve can be generated by testing the customer's equipment. A simple test is done by determining the time the equipment will continue to operate after a reduction of the voltage. The test is done for different levels of voltage reduction. The most simple voltage-tolerance curve will then be a coordinate in the magnitude-duration window, e.g. 100 ms, 65%. This coordinate is interpreted as follows: the equipment can withstand a voltage reduction to 0% of nominal voltage during 100 ms and also tolerate a voltage of 65% of nominal voltage indefinitely. This type of voltage-tolerance curve is called rectangular. More complicated, non-rectangular, voltage-tolerance curves can of course be generated.

2.6.1 Computers and consumer electronics

For computers special non-rectangular voltage-tolerance curves have been developed. Well known is the CBEMA curve and somewhat less known is the ITIC (or revised CBEMA) curve, both shown in Figure 2.12. It is recommended that computer equipment has a voltage-tolerance that is under these curves.

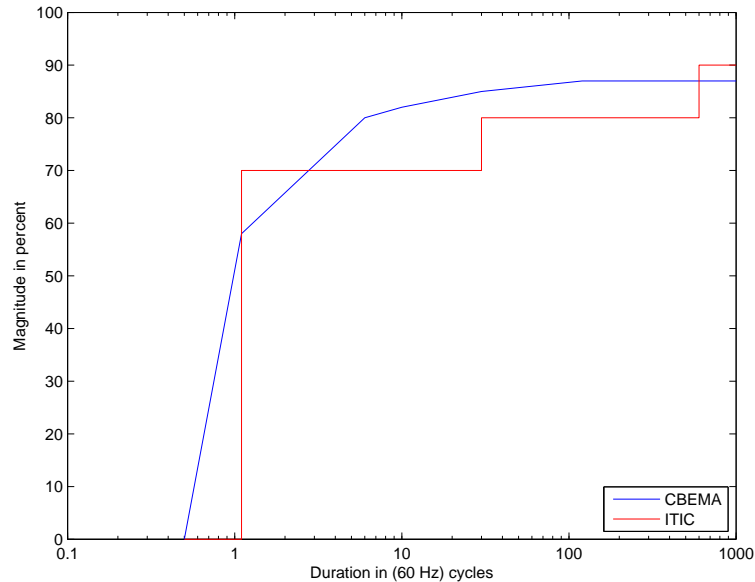


Figure 2.12: Voltage-tolerance curves according to CBEMA and ITIC. Data for the plot is taken from [4].

Computers and other consumer electronics are often powered using single-phase diode rectifiers. The rectified voltage can be regulated or un-regulated depending on the demands of the equipment. The voltage is filtered using a capacitor to eliminate ripple. Depending on the equipment's power demand and the size of the capacitor the immunity to voltage dips can vary. By installing a large hold-up capacitor the equipment can withstand longer dips.

2.6.2 Electric drives

Electric motors of both ac and dc type are often controlled by electronic equipment such as three-phase rectifiers and inverters using PWM. The drives are often equipped with protection to prevent the electronics and machines from damage. During a voltage dip the protection system can trip and the machine is disconnected. In some cases the machine is re-connected soon after the dip has ended, but often this is not possible, and there can be a substantial delay in operation or production. To retain the desired torque when the voltage drops there will be an increase in the current drawn. This over-current can lead to blown fuses or damage of the equipment.

The immunity of electric drives to voltage dips can be improved by different methods. By disabling the inverter in a adjustable speed ac drive the motor will not load the drive during the dip and over-currents can be disabled. By installing additional energy storage (capacitor banks or batteries) to the drive, tolerance against dips will increase. Three-phase dips require large

amounts of stored energy, but since most dips are of single-phase or phase-to-phase type that requires a limited amount of stored energy, this method can be affordable.

2.6.3 Directly fed induction motors

The majority of motors connected to the power system are still directly fed induction motors. These machines are rather insensitive to voltage dips but some problems can arise. At the end of a severe dip torque oscillations can occur that can lead to damage for the motor. When the voltage recovers after a dip there will be an increase of the current in the motor, first to rebuild the magnetic field in the airgap, then to accelerate the motor to the operating speed. This current increase can cause a post-fault dip with a duration of one second or more, which could lead to tripping of protection systems.

2.7 Economic costs due to voltage dips

The increase in the number of sensitive electronic equipment connected to the power system together with a demand for lean productions, result in an increase in the costs related to power quality problems. In recent years the attention towards the economic consequences of voltage dips has strengthened. It is of course difficult to make accurate estimations of the total costs related to voltage dips. A recommendation for an individual customer to estimate the economic consequences due to voltage dips and interruptions is found in [7]. Here the costs are divided into different categories like idled labor, lost production, cost to repair damaged equipment and cost of recovery. These are immediate consequences but also delayed costs can appear like increased labor costs due to downtime, lost business due to customer's dissatisfaction and fines and penalties due to delays.

In a survey made by Svenska Elverksföreningen 1994 to get an estimation of the customer's costs due to interruptions only interruptions longer than 3 minutes were considered. A more recent study (2004) also includes the economic consequences of voltage dips and the estimation done of the costs due to interruptions for year 2003 is given in Table 2.5. The costs are an estimation for all of Sweden. [8]

Table 2.5: Estimated costs of interruption 2003. [8]

Interruption time	Estimated cost
<3 minutes	1 000–1 500 MSEK
>3 minutes	1 400 MSEK
Total	2 400–2 900 MSEK

3 Existing software

As seen in the previous chapter voltage dips can cause severe problems with huge economic consequences for customers connected to a power grid. The interest in this aspect of power quality has increased over the past years due to more sensitive equipment and optimized production with small margins. To be able to estimate the number of dips a certain customer will experience, and their severity, a calculation software with sufficient accuracy is necessary. A calculation of the dip situation could then be a basis for decisions on improvements, both concerning the customer equipment and power system design.

A goal for this master thesis work is to improve the existing calculation software *Simpow Dips* by implementing capabilities to calculate dip durations and also a more accurate calculation of the dip magnitude. The current version of *Simpow Dips* produces a result-file in text-format containing information about the dips expected at selected locations. A fault is simulated at each one of the nodes in the system. For every fault the following information about the resulting dips at all nodes in the system is given:

1. Number of faults per year divided into three-phase, two-phase-to-ground, phase-to-phase and single-phase-to-ground faults
2. For each fault type, the dip type, characteristic voltage, PN factor and zero-sequence voltage, all in complex format

Some limitations in the software where improvements could be made are obvious. The following points were to be treated during the master thesis work:

1. Only information about the magnitude of the dip is handled in the existing version. Even if the magnitude is sufficient to calculate affected and exposed areas [9] in a power system the dip duration is of high interest to estimate how customers are affected and as a basis for improvements.
2. Even if fault-frequencies for lines are given as input to the software, faults are in the existing version not simulated at the lines but rather at the nodes connected to the line. Theories exist on how to calculate characteristic voltage at nodes for faults occurring at lines but are not implemented in the existing version of *Simpow Dips*.
3. Different graphical presentations of the dip situation have been suggested in textbooks and standards. A graphical output of the result from *Simpow Dips* would greatly enhance the readability.

As verification of the software accuracy it is desirable to compare recorded measurements of dip events at a certain bus in a power system with calculations of the same system.

4 Improvements in the software

In this chapter a detailed description is given of the methods used to fulfill the project and solve the problems outlined in Chapter 3. The work can be seen as divided in three parts, which will be handled separately: calculation of dip duration, improved calculation of dip magnitude and graphical representation of the calculation result.

4.1 Calculation of dip duration

Even though the fault-clearing time intuitively is considered a deterministic value depending on the protection system in use and its time delay settings, the actual fault-clearing times seen by the customers can deviate considerably from these design values. Different approaches are possible in the choice of model to calculate the dip duration as a result of a fault.

A method that requires substantial work but probably delivers the most reliable results is to take into account each individual protection relay throughout the system with its setting. For a fault at a given position, information about the involved protection relay (or relays) will give knowledge about the dip duration as a result of the fault. An exact value can however not be given for a number of reasons:

1. Relay operating time depends on fault current which cannot be exactly foreseen
2. Circuit breaker interruption time can vary
3. A protection relay or circuit breaker can malfunction and thus increase the fault-clearing time considerably

The consequence is that at best a narrow time interval can be given as estimation for the dip duration (see also Table 2.4!). This drawback of the method together with the considerable work to collect information on each protection relay calls for another approach.

Another method is to divide the power system of interest into smaller subsets, each one with the same stochastic characteristics of dip duration. Instead of a fixed fault-clearing time or dip duration for each fault position, a probability distribution function for a (large) group of fault positions is assumed. This probability distribution includes a range of uncertainties, including variations in relay settings, fault current, fault location compared to the relay and failures of the protection.

A natural division would be voltage levels, since the choice of protection system, and thus, the fault-clearing time, is strongly connected to the voltage level. This is of course a simplification of the problem, but especially for higher voltage levels, i.e. transmission levels, it seems acceptable, due to a high degree of control and high demands. Since settings in lower voltage level protection systems can vary to a greater extent, especially for radial systems, it will need a more careful consideration.

As a basis for obtaining a probability distribution of dip durations, knowledge of the protection system at each voltage level could be used during the calculations. For example Table

2.4 could serve as data for each voltage level when performing calculations for that particular power system. A drawback with this approach is that actual dip durations experienced at the busses throughout the system can deviate from these settings.

An alternative basis for obtaining the probability distributions could be recorded measurements of dip events in the system of interest or one with equal characteristics. Especially for transmission levels this would produce accurate data, since the dip duration profile for the transmission system is homogenous in the grid. In Figure 4.1 magnitude-duration characteristics for a large amount of measured dip events in a power system with different voltage levels—MV (medium voltage), HV (high voltage) and EHV (extra high voltage)—are shown (these measurements are used in Chapter 10 in [10]). Note that the events in the figure are *recorded* at different voltage levels. In this data there is no information about at what voltage level the fault occurred that resulted in the dip. This does not make the recordings useless. It can be shown that faults produce shallow dips for voltage levels higher than the fault level, e.g. a fault on a HV line does not cause a serious dip at EHV level. This is because of the damping effect of transformer impedances. Making use of this information can lead to a better interpretation of the data.

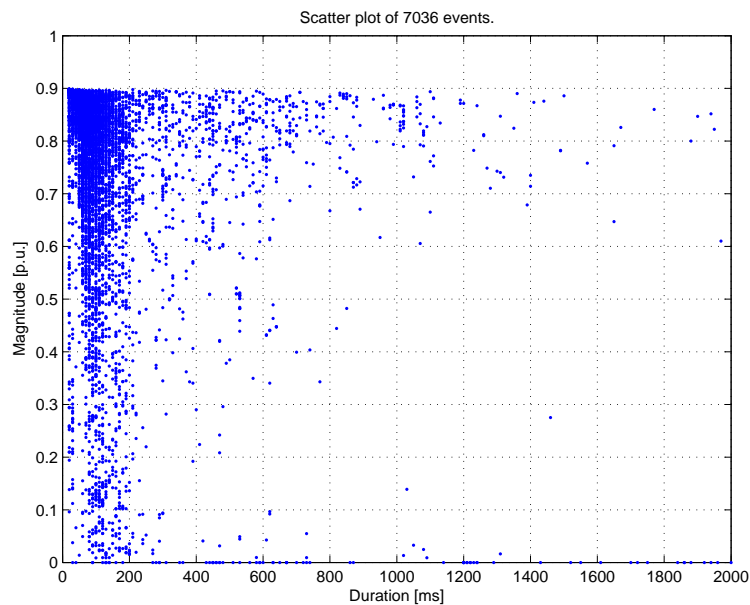


Figure 4.1: Example of recorded measurements of dip events. This is an aggregation of all sites at all voltage levels.

The data shown in Figure 4.1 can further be divided to contain only events recorded at the specific voltage levels. Individual scatter plots for each voltage level are found in Figure 4.2 through Figure 4.4. A second plot for each voltage level also contains the PDF (probability distribution function) and pmf (probability mass function) to get a more qualitative picture of the distribution. Observe again that recorded events at a certain voltage level also contain dips due to faults at higher voltage levels. As we move to lower voltage levels dip data is the cumulated results of faults occurring at different voltage levels. Also observe that the number of monitors are not the same at the different voltage levels (this explains the large variation in the number of recorded events at each voltage level) and that a monitor location at a higher voltage level not always corresponds with a monitor location at a lower voltage level.

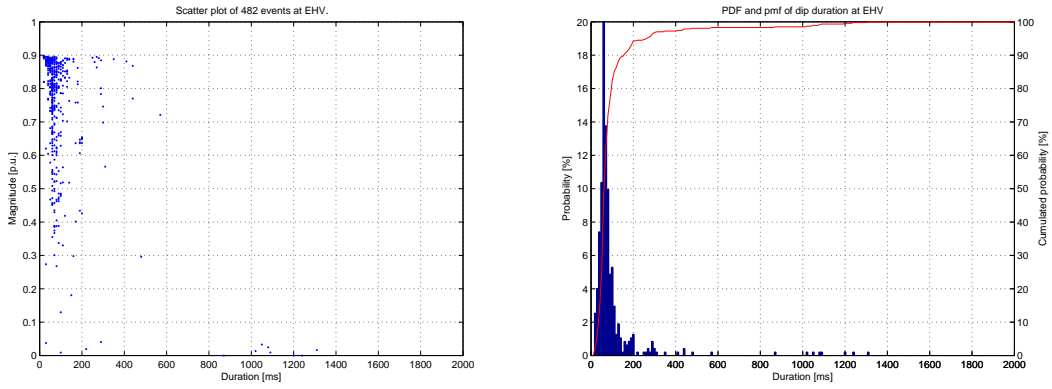


Figure 4.2: Scatter plot and distribution of dip durations for fault recorded at EHV.

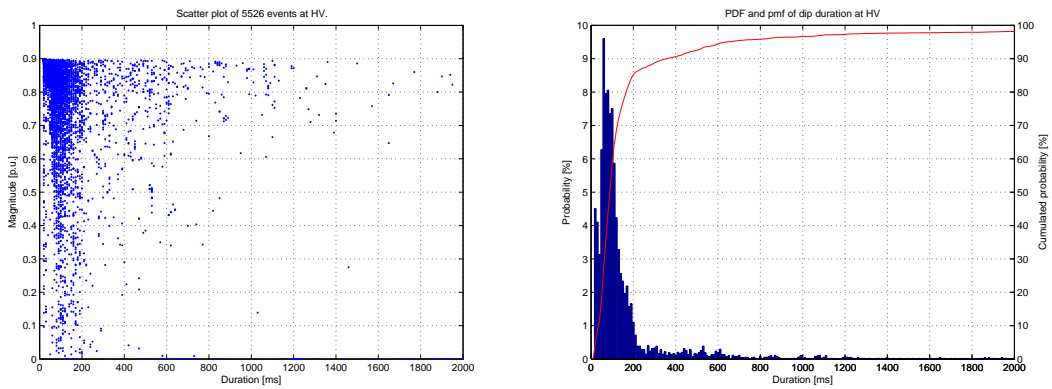


Figure 4.3: Scatter plot and distribution of dip durations for faults recorded at HV.

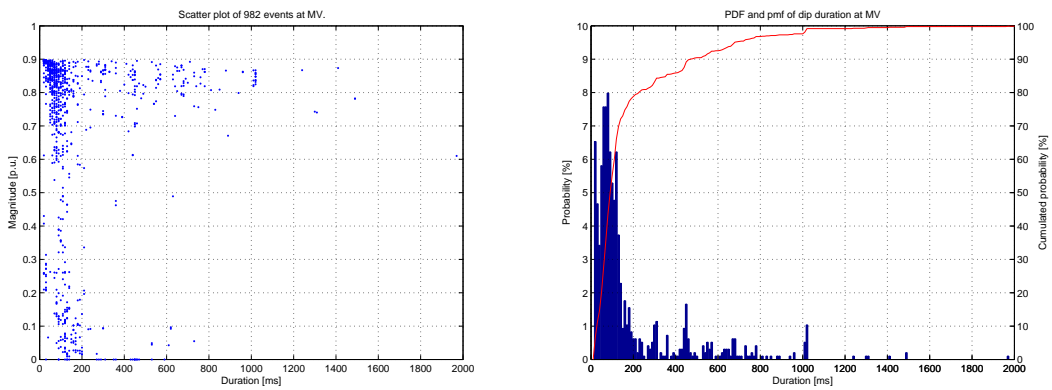


Figure 4.4: Scatter plot and distribution of dip durations for faults recorded at MV.

In Figure 4.5 through Figure 4.7 an attempt is made to filter out faults from higher voltage levels. For each dip duration the value from the pmf in the higher voltage level is subtracted from the corresponding value in the lower voltage level. It has been taken into considera-

tion that the number of monitors is different at each voltage level. For the method to be valid, recorded events at the different voltage levels must have taken place in the same system, and this assumption is made. Furthermore, the values have been filtered using Matlab's `filter`-function (a transposed direct-form II IIR filter).

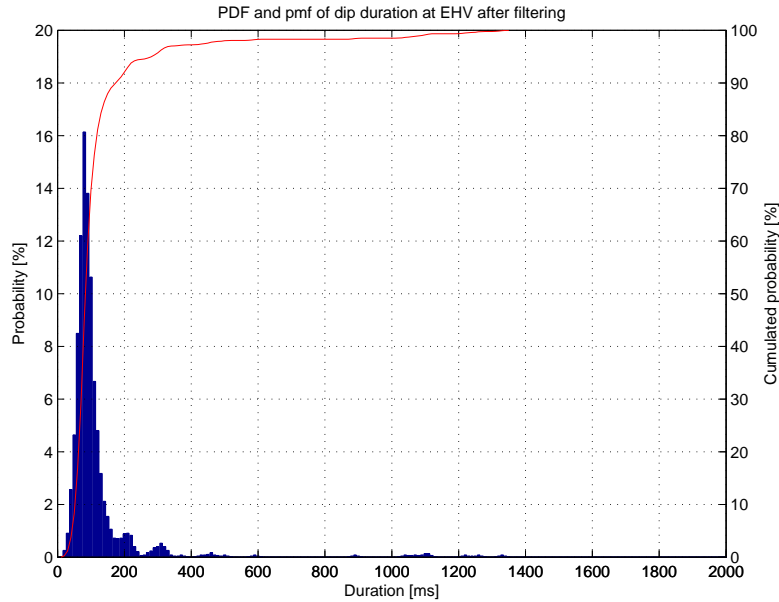


Figure 4.5: Distribution of dip durations for faults originating at EHV.

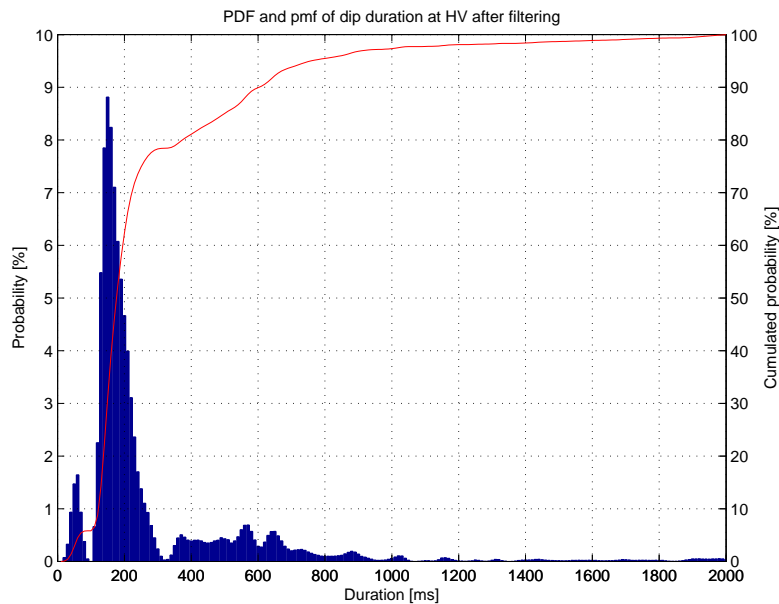


Figure 4.6: Estimated distribution of dip durations for faults originating at HV.

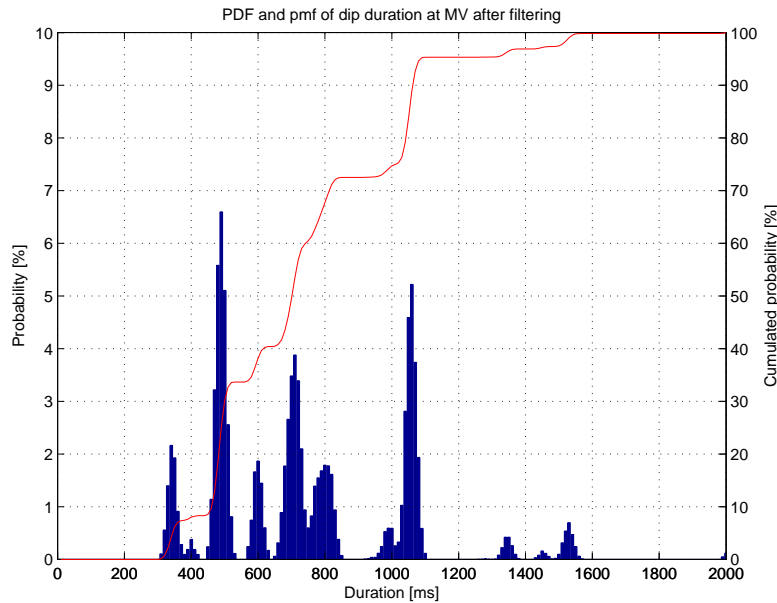


Figure 4.7: Estimated distribution of dip durations for faults originating at MV.

To accurately interpret the data in previous figures it is convenient to also have information about the protection systems used. Especially for lower voltage levels with radial distribution this would be helpful since overcurrent relays are often used and the coordination schemes have unique settings for each area.

Regardless of the method used to achieve the probability distribution function of the dip duration for each voltage level, the software should be able to perform a sufficient calculation. With the discussion above as basis for a model the following software implementation was chosen:

1. For each voltage level the faults are cleared—and thus the dip duration will be—in one or more *duration zones*. These zones do not have to correspond to the protection zones used in relay settings. Two or three duration zones are expected to be sufficient for each voltage level.
2. Assume a *triangular distribution* of the dip durations in each duration zone.
3. For each duration zone there is a *probability* that the dip duration occurs in that particular zone.
4. To achieve a triangular distribution a *minimum*, *maximum* and *typical value* of the dip duration is chosen for each duration zone.

EXAMPLE 4.1 Consider a meshed power system at EHV as in Figure 4.8. The bus where an estimation of the dip situation is needed is bus number 3. Faults are assumed to occur only on busses number 1 and 2.

Also assume that the characteristics for dip duration are as in Figure 4.5. After analyzing the distribution it is concluded that dip occur in two duration zones with the following parameters:

1. Probability: 93%, minimum duration: 20 ms, typical duration: 80 ms and maximum duration: 160 ms.

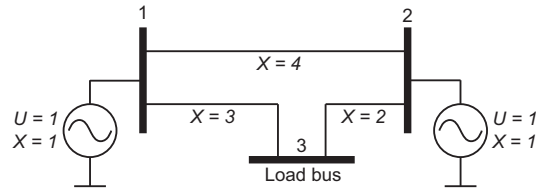


Figure 4.8: Simple meshed power system at EHV.

2. Probability: 4%, minimum duration 250 ms, typical duration: 290 ms and maximum duration: 360 ms.

The distribution is shown in Figure 4.9 for clarification. Further assume a fault-frequency of one fault per year for each of the different fault types at busses 1 and 2.

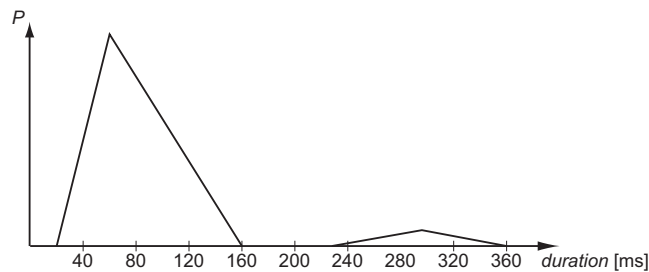


Figure 4.9: Distribution of dip durations at EHV used for calculation.

In Figure 4.10 the result of a calculation over 20 years for the situation at bus number 3 is given as a scatter plot. (This kind of representation and how it is produced is explained later in this chapter, but the result is given here for illustration.) The two different time zones can be clearly seen in the scatter plot with the individual dip event durations triangularly distributed. Observe that four distinctive dip magnitudes are present. Faults at busses number 1 and 2 result in dips of different magnitude. Dips as result of single-phase-to-ground faults are of less magnitude, separating those dips from the ones resulting from other fault types.

■

The following subsection will describe the implementation of the model discussed above in Simpow Dips.

4.1.1 Implementing the model in Simpow Dips

Since Simpow Dips is an existing software complementing Simpow, addition of new features needs some consideration. It is a good practise in object oriented programming (the software is developed using C++) to re-use ready-made functions and to adapt the added code to the existing as transparent as possible. Therefore a good understanding of the program layout and execution is necessary. Modifications are preferably made in small steps to enable debugging and control of function.

As a first modification a simplified estimation was used to calculate the dip duration. The dip duration was modelled as a function of the voltage level where the fault occurred. The fault-clearing times in Table 2.4 were plotted against the voltage level and an exponential function

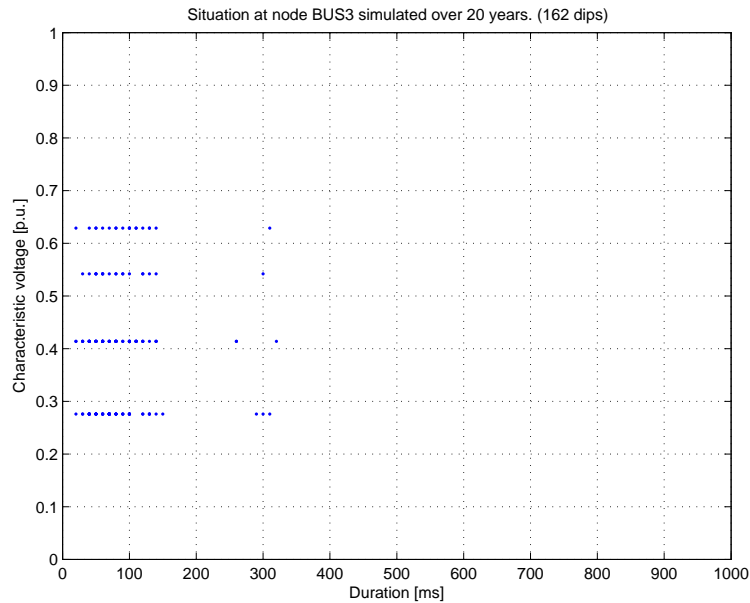


Figure 4.10: Calculation of the dip situation at bus 3 represented as a scatter plot.

was fitted to the data points. The result is shown in Figure 4.11. In *Simpow Dips* the voltage level for each bus in the power system is stored. Thus this way of addressing the problem was easy to implement. Faults cleared by second or third zone protection relays when using distance protection were not considered, nor time delay when using overcurrent relays.

The existing version of *Simpow Dips* creates a result-file containing dip magnitude at each node in the system for a fault occurring at each node at a time. With the modelling of the dip duration introduced above, the result-file also contains the dip duration in ms for each fault location.

A second modification of the software required more extensive programming. As input to the existing version of *Simpow Dips* a fault-information file is required. This file consists of two sections: fault-frequencies for the individual nodes in the system and fault-frequencies for the lines connecting the nodes. By modifying *Simpow Dips* the software also reads a third section in the fault-information file: dip duration for each existing voltage level in the system. This enables the user to control the distribution of the durations. In Figure 4.12 a simple fault-information file is shown.

The data in the file is interpreted as follows:

NODE The first column identifies the node of interest. The second through fifth columns give the fault frequencies for three-phase, two-phase-to-ground, phase-to-phase and single-phase-to-ground faults in faults per year.

LINES The first and second column identify to which nodes the line is connected. The third column gives the individual line name since several parallel lines can exist between the nodes. Columns four through seven give the fault frequencies for three-phase, two-phase-to-ground, phase-to-phase and single-phase-to-ground faults in faults per year and km.

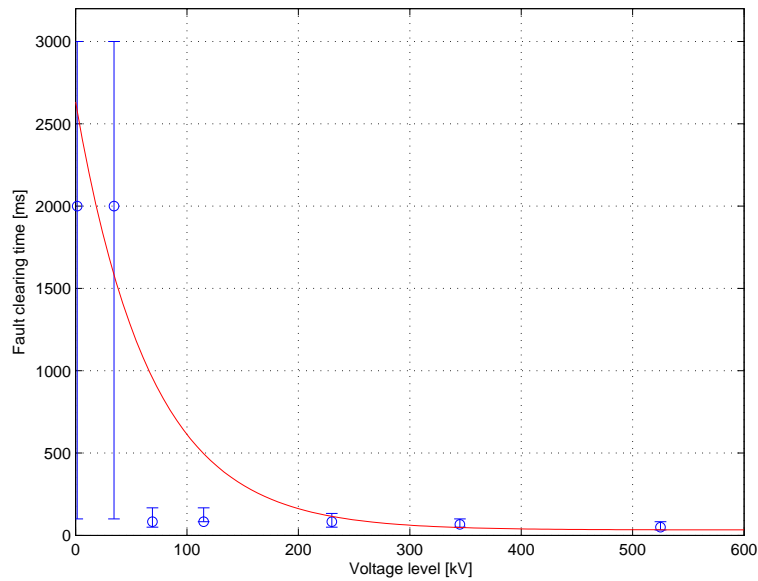


Figure 4.11: Fitting of exponential function to fault-clearing times.

NODE								
795166	0.25	0.20	0.14	0.30				
795178	0.15	0.25	0.10	0.30				
795190	0.4	0.19	0.04	0.31				
795206	0.112	0.26	0.141	0.305				
795218	0.4	0.19	0.04	0.31				
795230	0.15	0.25	0.10	0.30				
795242	0.25	0.20	0.14	0.30				
795254	0.4	0.19	0.04	0.31				
END								
LINES								
795166	795178	1	0.91	1.25	0.93	1.24		
795178	795190	1	0.91	1.25	0.93	1.24		
795190	795206	1	0.91	1.25	0.93	1.24		
795218	795230	1	0.91	1.25	0.93	1.24		
795230	795242	1	0.91	1.25	0.93	1.24		
END								
DURATION								
0.4	0.66	20	60	300	0.33	300	1000	2000
20	0.79	20	60	200	0.19	200	500	1000
400	0.93	20	80	160	0.04	250	290	310
END								

Figure 4.12: Example of fault-information file.

DURATION The first column gives the voltage level in kV. Column two gives the probability of dip duration occurring in duration zone 1. Columns three through five give the minimum, typical and maximum dip durations for duration zone 1. Columns six through nine give the same information for duration zone 2.

Since each node in the system has a nominal voltage level, information of the corresponding duration distribution has to be assigned to the node. This required some new class variables to be added. The output to the result-file also had to be modified to include information about the duration. An excerpt from a result-file is shown in Figure 4.13 where the dip duration information is seen for bus 795166.

8						
Fault pos./Nodes	3-phase faults			PNF.	Zseq.	
	Dip type	C.V.				
795166						
Zone 1 probability: 0.79						
Zone 1 lower limit: 20						
Zone 1 typical value: 60						
Zone 1 upper limit: 200						
Zone 2 probability: 0.19						
Zone 2 lower limit: 200						
Zone 2 typical value: 500						
Zone 2 upper limit: 1000						
Fault freq. [faults/year]	0.000					
795166	A	0.000	90.0	0.000	90.0	0.000
795178	A	0.000	155.3	0.000	155.3	0.000
795190	A	0.000	155.3	0.000	155.3	0.000
795206	A	0.000	155.3	0.000	155.3	0.000
795230	A	0.983	-0.1	0.983	-0.1	0.000
795218	A	0.983	-0.1	0.983	-0.1	0.000
795242	A	0.983	-0.1	0.983	-0.1	0.000
795254	A	0.000	-5.2	0.000	-5.2	0.000

Figure 4.13: Example of result-file.

With this method implemented, all information is available in the result-file to analyze the dip magnitude-duration situation at the busses in the system.

4.2 Improved calculation of dip magnitude

The second topic for the master thesis project is to improve the calculation of dip magnitude in Simpow Dips. As seen in Figure 4.12, fault information is given both for nodes and lines. In reality most faults appear along the lines and not in the components placed in the nodes (busbars, transformers, breakers, disconnectors, etc.). In the existing version of Simpow Dips the fault-frequency of a line is divided in two and each one of the nodes connected to the line get an increased fault-frequency. The following example illustrates this.

EXAMPLE 4.2 Assume that a line of length 10 km and a fault-frequency of 1 fault per year and km is connected to nodes *A* and *B*. Node *A* has a fault-frequency of 0.1 fault per year and node *B* has a fault-frequency of 0.2 faults per year. The line is divided in two parts of 5 km each, with fault-frequencies of 5 faults per year each. These frequencies are added to nodes *A* and *B*. Thus, *A* obtains a fault-frequency of 5.1 faults per year and node *B* obtains a fault-frequency of 5.2 faults per year.

■

Since each line has an impedance we can conclude that a fault on a line close to a generating bus will cause a larger fault-current than a fault on the same line far from the generating bus. On the other hand, we conclude that a fault on a line close to a load bus will cause a smaller fault-current than a fault on the line far from the load bus. By moving the faults (as is done in the existing version of Simpow Dips) to the nodes the fault-currents are either under- or over-estimated. Also consider the model in Figure 2.6. Moving the fault location to PCC or the node at the other end of the faulted line will affect the value of the impedance to fault, Z_F , and thus the dip magnitudes are miss-calculated.

In the following subsection, a method to calculate the dip magnitude for a fault along the line, taking into account the line-impedance, is presented.

4.2.1 Description of Moving Fault Node method

This method is described in detail in [9] and [11] for balanced dips (due to three-phase faults) but will be discussed here also with respect to unbalanced dips. Consider the system in Figure 4.14 consisting of two generator busses, j and k , and a load bus, m , for which we are interested in the dip magnitude resulting from a fault between j and k .

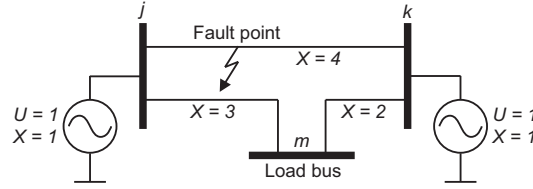


Figure 4.14: Model to illustrate Moving Fault Node method.

The during-fault voltage at bus m will be

$$U_m = U_{m0} - \frac{Z_{mf}}{Z_{ff}} U_{f0} \quad (4.1)$$

where U_{m0} and U_{f0} are the pre-fault voltages at bus m and at the fault position respectively, Z_{mf} is the transfer impedance between bus m and the fault position and Z_{ff} is the source impedance at the fault position.

Parameters involving the fault position require knowledge of the distance to nodes j and k . A parameter, λ , is therefore introduced. The value of λ ranges from 0 to 1. With $\lambda = 0$ the fault occurs at bus j and with $\lambda = 1$ the fault occurs at bus k . We can now define

$$U_{f0} = U_{j0} + \lambda (U_{k0} - U_{j0}) \quad (4.2)$$

$$Z_{mf} = Z_{mj} + \lambda (Z_{mk} - Z_{mj}) \quad (4.3)$$

$$Z_{ff} = Z_{jj} + \lambda (2Z_{jk} - 2Z_{jj} + z_{jk}) + \lambda^2 (Z_{jj} + Z_{kk} - 2Z_{jk} - z_{jk}). \quad (4.4)$$

In (4.4) the line impedance between busses j and k is used, z_{jk} . Observe that all parameters containing the fault position, f , in (4.1) now can be expressed using voltage and impedance information for the busses in the system with addition of the parameter λ , describing where on the line the actual fault occurs. The required information is easily fetched in Simpow Dips.

EXAMPLE 4.3 To illustrate the method it is applied to the system in Figure 4.14. (4.1) is calculated for values of λ between 0 and 1. The result is plotted in Figure 4.15. ■

The method above is here applied to the balanced situation but can be adapted to unbalanced faults and used to calculate the characteristic magnitude. Calculations are made using symmetrical components and (4.3) and (4.4) can be used to calculate negative and zero sequence impedances, $Z_{ff}^{(2)}$, $Z_{mf}^{(2)}$, $Z_{ff}^{(0)}$ and $Z_{mf}^{(0)}$ by replacing each impedance with its negative or zero sequence equivalence.

To calculate the characteristic magnitude both positive and negative sequence during-fault voltage is needed. For the different fault types the sequence voltages are derived as follows.

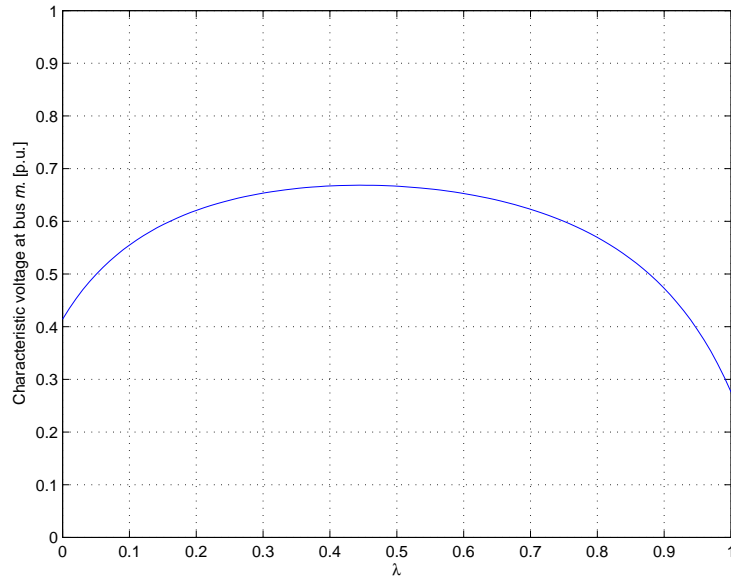


Figure 4.15: During-fault voltage at bus m for different fault positions.

Two-phase-to-ground fault:

$$U_m^{(1)} = U_{m0} - \frac{Z_{mf}^{(1)} (Z_{ff}^{(0)} + Z_{ff}^{(2)})}{Z_{ff}^{(0)} (Z_{ff}^{(1)} + Z_{ff}^{(2)}) + Z_{ff}^{(1)} Z_{ff}^{(2)}} U_{f0} \quad (4.5)$$

$$U_m^{(2)} = \frac{Z_{mf}^{(1)} Z_{ff}^{(0)}}{Z_{ff}^{(0)} (Z_{ff}^{(1)} + Z_{ff}^{(2)}) + Z_{ff}^{(1)} Z_{ff}^{(2)}} U_{f0} \quad (4.6)$$

Phase-to-phase fault:

$$U_m^{(1)} = U_{m0} - \frac{Z_{mf}^{(1)}}{Z_{ff}^{(1)} + Z_{ff}^{(2)}} U_{f0} \quad (4.7)$$

$$U_m^{(2)} = \frac{Z_{mf}^{(2)}}{Z_{ff}^{(1)} + Z_{ff}^{(2)}} U_{f0} \quad (4.8)$$

Single-phase-to-ground fault:

$$U_m^{(1)} = U_{m0} - \frac{Z_{mf}^{(1)}}{Z_{ff}^{(1)} + Z_{ff}^{(2)} + Z_{ff}^{(0)}} U_{f0} \quad (4.9)$$

$$U_m^{(2)} = -\frac{Z_{mf}^{(2)}}{Z_{ff}^{(1)} + Z_{ff}^{(2)} + Z_{ff}^{(0)}} U_{f0} \quad (4.10)$$

For calculation of the characteristic magnitude from positive and negative sequence voltages it is referred to Table 2.3.

EXAMPLE 4.4 Example 4.3 is here repeated for unbalanced faults and the result is plotted in Figure 4.16. Observe that single-phase-to-ground faults result in significantly higher characteristic magnitude (thus less severe dips) than other fault types as mentioned earlier in Section 2.3.

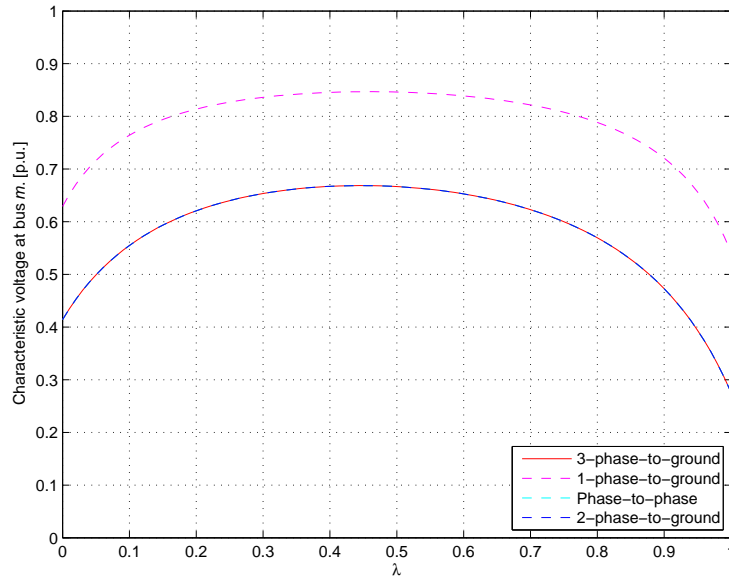


Figure 4.16: Characteristic voltage at bus m for different fault types.

■

Distribution of λ

The parameter λ describes the actual position for a fault along a line. As input data in the fault-information file only the fault-frequency for each line is given (number of faults per year and km). No information is given for the fault positions along the line. Some statistical distribution of the fault positions must be made to perform the calculation. A simple and not unrealistic approach is to use a uniform distribution of λ between 0 and 1. This corresponds to the probability for a fault to occur being equal all over the line. For very long lines this is not true since the risk of lightning, for example, can differ substantially along the line. A solution to this problem is to introduce one or more fictive nodes along the line, thus dividing it into shorter lines with different fault-frequencies.

EXAMPLE 4.5 Consider again the system in Figure 4.14 with faults occurring both at busses j and k and along the line between those busses. The faults along the line are assumed to be uniformly distributed. The result of a calculation is shown in Figure 4.17. (This kind of representation and how it is produced is explained later in this chapter, but the result is given here for illustration.) Blue dots represent dips due to faults in the busses and red dots represent dips due to faults along the line. It can be concluded that the majority of the faults along the line will result in dips with magnitudes over 0.5 p.u. In this case the method of Moving Fault Node will give a much more accurate picture of the dip magnitudes than assuming that all

faults occur in the busses. Observe that only balanced three-phase faults have been simulated in this example.

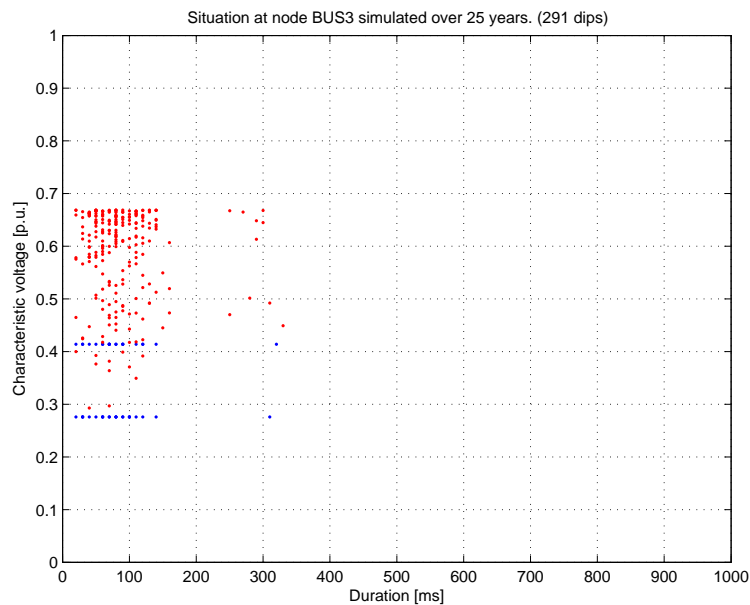


Figure 4.17: Dip situation at bus m using Moving Fault Node method.

■

4.2.2 Implementing of Moving Fault Node method in Simpov Dips

Information about fault-frequencies is given in the fault-information file, both for nodes and lines. Modifications had to be done in handling the information. In Simpov Dips an object is made for each network component that can experience a fault, a `FaultNodeElement`. To simulate faults on lines a class called `FaultLine` was defined. For objects of this class, certain variables were defined to be able to calculate (4.3) and (4.4): line length, resistance and reactance were fetched from the information about the network system and fault-frequencies and distribution of the dip durations were fetched from the fault-information file. The information needed to analyze the dip magnitude-duration situation at the busses is printed in the result-file.

4.3 Graphical representation of the result-file

Since Simpov Dips has no support for graphical output and delivers a text-format result-file an analysis program was made in Matlab to read the result-file and plot information of interest. As input to the program is given

1. The result-file from Simpov Dips
2. The name of the bus where the dip situation is to be calculated
3. Number of years to simulate

In textbooks and standards different representation methods have been proposed ([4] and [7]). The purpose of the different graphs is to get a good qualitative and quantitative estimation of the dip situation and also to be able to compare it to the customer's immunity. Here follows a description of the different plots produced by the Matlab analysis program.

4.3.1 The scatter plot

To get a good view of the voltage dip situation for a certain customer, the measured or expected dips are plotted in a magnitude-duration window. Each dip event is characterized by its two main features: the magnitude (or characteristic voltage) and the duration, and plotted as a point in the magnitude-duration window. The result is also called a *scatter plot*. With information about a large number of events—by monitoring for a long period of time or using calculation with statistical information about the power system—it is possible to make decisions about improvements of the power suppliers and/or customers equipment. The Matlab analysis program produces a magnitude-duration plot with faults of different types separated by colour. An example is seen in Figure 4.18.

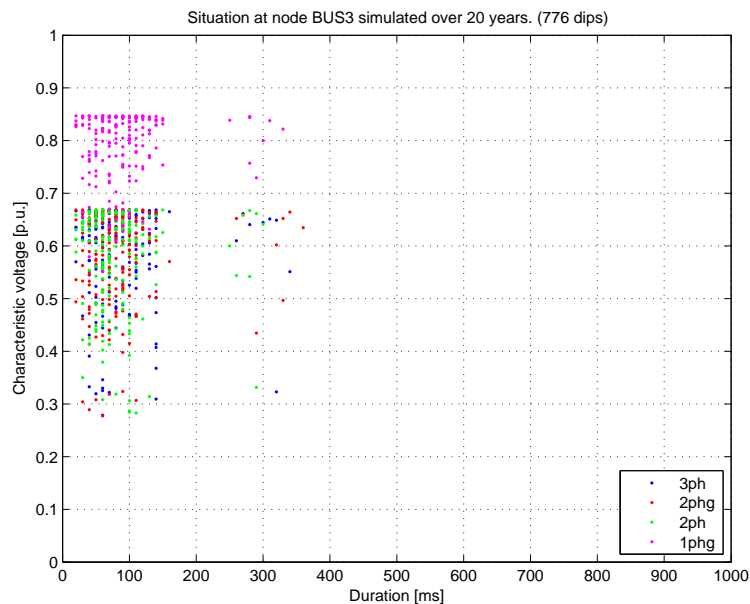


Figure 4.18: Combined scatter plot of all dip types.

The number of events plotted in the scatter plot is decisive for its readability and usefulness. Too few events will prevent the reader from drawing any conclusions and too many events will result in a clogged scatter plot with the same consequence. If the scatter plot is used to present monitored events, the monitoring time must be long enough to produce a sufficient number of events. If the fault-frequencies are low in the monitored network a monitoring time of several years will be necessary. When making calculations using the Matlab analysis program the time period of simulation can be chosen to produce the sufficient number of dips.

When creating the different plots one need to consider the number of years to simulate over. This depends on the type of plot and also on the different fault-frequencies of the components in the network. Different simulation times can be needed for different kind of plots. For a scatter plot around 1 000 events will give an informative picture of the situation. In general a

simulation over a few hundred years is sufficient, but this may result in a very clogged scatter plot in case of high fault-frequencies.

To further increase the readability of the scatter plot an alternative plot where the four fault types are separated in individual graphs is produced. An example is shown in Figure 4.19.

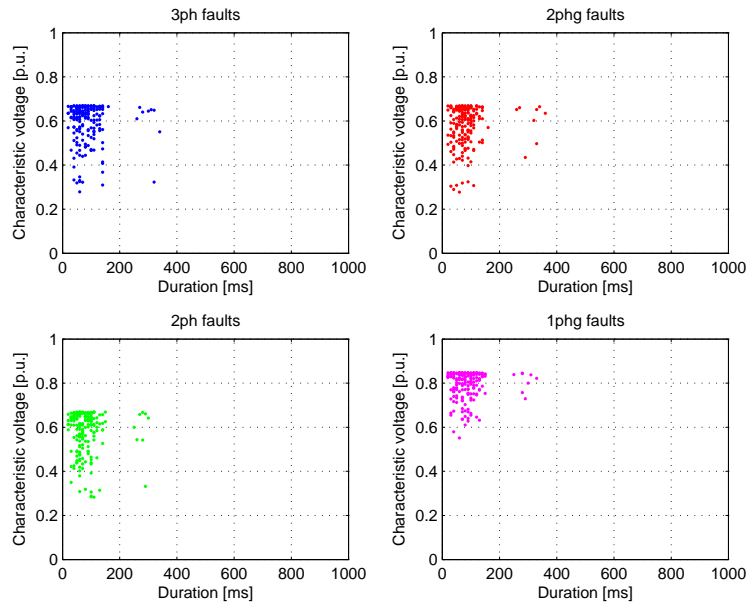


Figure 4.19: One scatter plot for each fault type.

4.3.2 The voltage dip coordination chart

To make use of the magnitude-duration plot it is important for the customer to have knowledge about its equipment or process immunity to voltage dips, i.e. for a certain dip magnitude what is the maximum duration the equipment can withstand. By plotting this for several different dip magnitudes, a voltage-tolerance curve is created showing the customers immunity to voltage dips. A simple representation of the immunity is a rectangle in the magnitude-duration window growing from the lower right corner. Dip events inside this rectangle cause a production stop or damage to equipment. Dip events outside the rectangle are harmless. Extensive information on how to create and interpret these voltage-tolerance curves is given in [7].

Instead of counting the number of dip events inside the rectangle (or more complicated area) curves representing the number of dips can be plotted. Along each curve the number of dip events are constant—the lines become iso-contours. This kind of representation is called a *voltage dip coordination chart*. If the equipment immunity is represented by a rectangle the number of dip events inside the rectangle are equal to the iso-contour at the upper left corner of the rectangle. Thus, the number of production stops is easily appreciated. The Matlab analysis program produces such a coordination chart and an example of this is shown in Figure 4.20. To produce a reliable coordination chart the time span of the simulation must be large (preferably some hundred years).

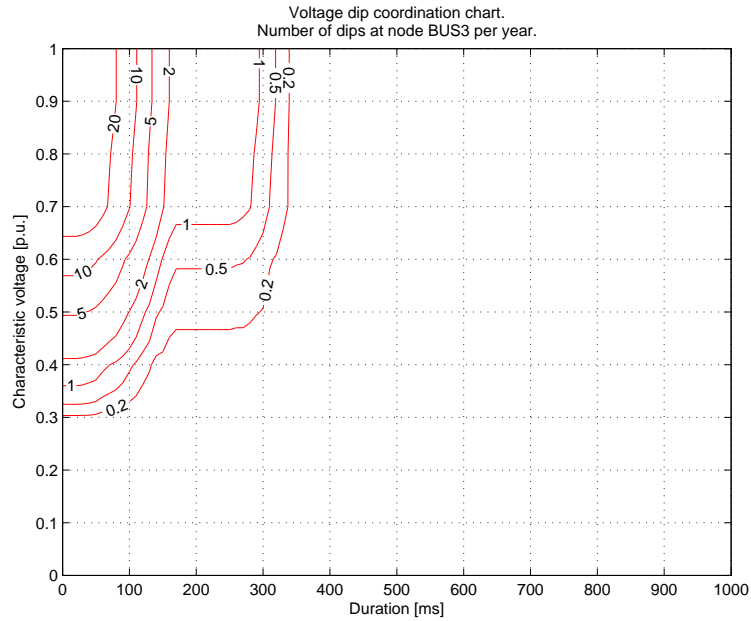


Figure 4.20: Voltage dip coordination chart of the situation at the bus.

4.3.3 The voltage dip density chart and cumulative voltage chart

The Matlab analysis program produces two plots of qualitative use: a *voltage dip density chart* and *cumulative voltage dip chart*, as seen in Figure 4.21 and Figure 4.22. In the dip density chart the magnitude-duration window is divided into a grid of low resolution and the number of dips in each slot is counted on a per-year basis. The plot is three-dimensional for readability. The cumulative chart uses the same grid but the number of dips is cumulated in each slot when moving towards shorter duration and higher magnitude. As for the coordination chart it is important to simulate over a large time span to achieve reliable charts of this type.

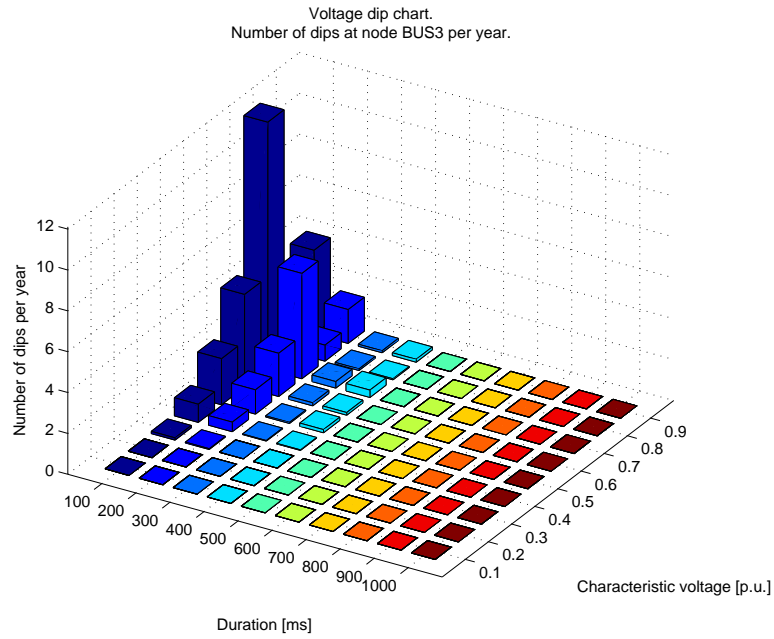


Figure 4.21: The voltage dip density chart of the situation at the bus.

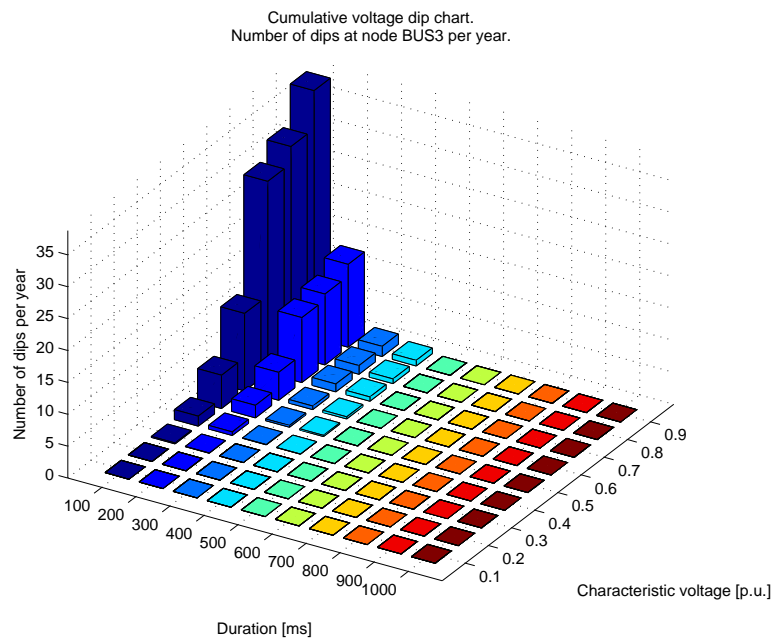


Figure 4.22: The cumulative voltage dip chart of the situation at the bus.

5 Applying the improved software to a realistic network

In this chapter Simpow Dips with the additions discussed above will be used to perform calculations on a simple but realistic power network. The system as shown in Figure 5.1 consists of 22 nodes and 26 lines on three different voltage levels: 400, 130 and 40 kV (the 40 kV part of the network is minor but is included since it is close to the bus of interest). In a previous master thesis, [12], an extended version of this network was used for a similar analysis and a comparison between the results in these two reports could be done. In [12] only dips due to three-phase faults are considered and a more deterministic approach to the problem is taken.

In the calculations to follow bus number 1306 in the bottom left of Figure 5.1 is taken as customer connection, where the dip situation is to be estimated. To show the advantage of the calculation approach, the effects on the dip situation will be studied for some changes in the network.

5.1 Fault-frequencies

In statistical reports fault-frequencies are often identified with its cause (lightning, external influences, maintenance, technical equipment, etc.) rather than divided into fault types. Studies have been made ([13] and [14]) to determine the probability of each fault type and these have been used as a basis for the calculations shown here. For the total number of faults per year and km at each voltage level, the data in [12] has been used. Fault-frequencies are summarized in Table 5.1. At subtransmission levels (130 kV) both shielded and unshielded lines are in use. The presence of shielding wires can alter the probability of the different fault types, [13]. This has been taken into consideration for this calculation. Faults are assumed to occur only on lines and thus the fault-frequencies for all nodes are set to zero.

Table 5.1: Fault-frequencies used in calculations.

Voltage level	Number of faults	3-phase	2-ph-gnd	2-phase	1-ph-gnd
400 kV	0.0042 (km yr) ⁻¹	9.5%	8.5%	2%	80%
130 kV unshielded	0.03 (km yr) ⁻¹	80%	0%	10%	10%
130 kV shielded	0.0225 (km yr) ⁻¹	53%	22%	5%	20%
40 kV	0.0356 (km yr) ⁻¹	7%	4%	23%	66%

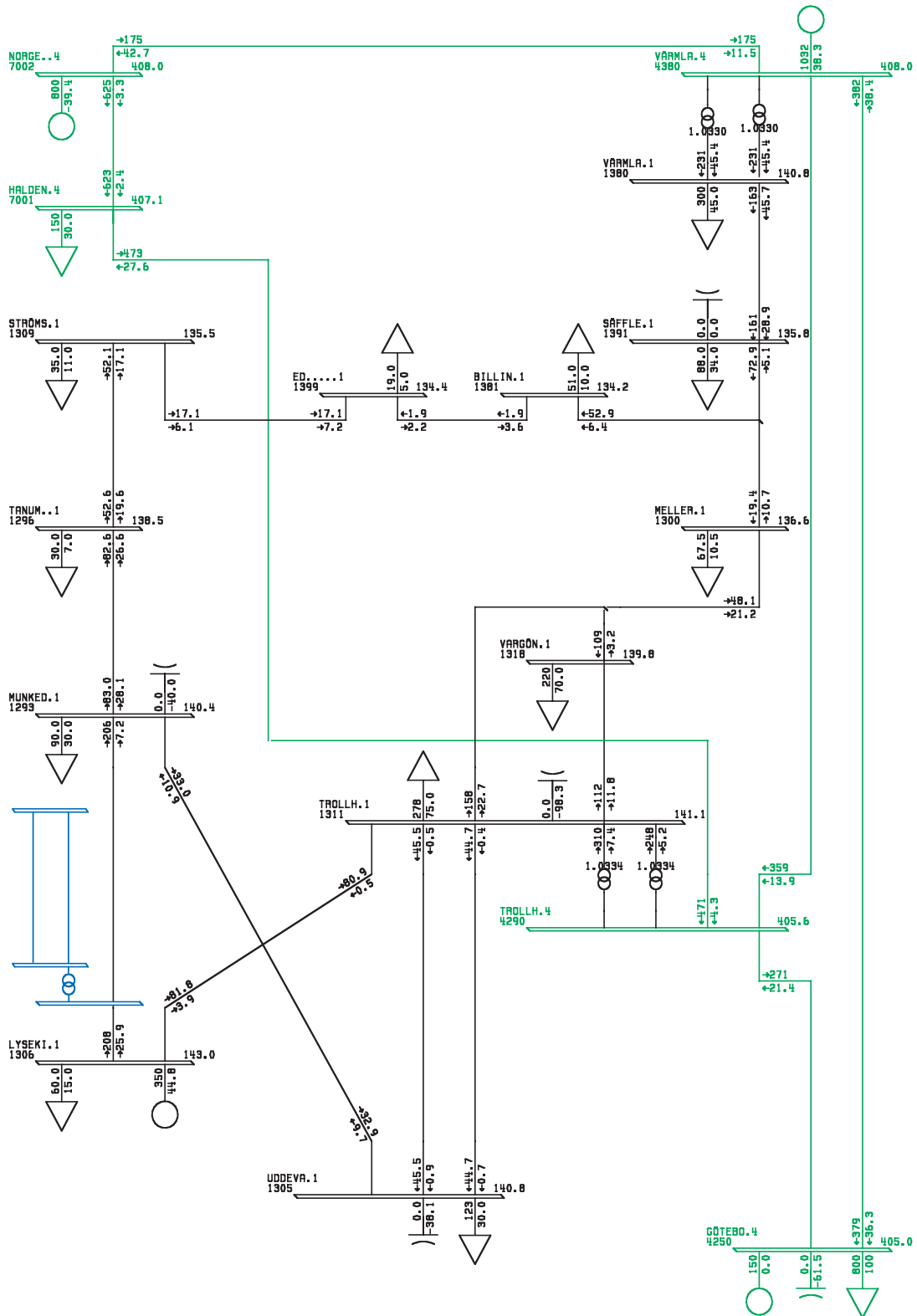


Figure 5.1: Network used for calculations. Green areas are 400 kV, black are 130 kV and blue are 40 kV.

5.2 Dip duration distributions

It was argued above that a combination of measurements and knowledge of the settings of the protection systems used in the network gives the best input data to the calculation of dip durations. For the network of interest no measurements are available. For the first calculations, data from the earlier study on this network is used as input, [12]. Table 5.2 gives the dip duration distributions used for these calculations. The calculation results when using these distributions are presented and discussed in Section 5.3. In the subsections that follow the effects of different changes to the network are calculated and discussed.

Table 5.2: Distribution of dip durations according to [12]. (Times in ms.)

Voltage level	P _{dur. zone 1}	Min.	Typ.	Max.	P _{dur. zone 2}	Min.	Typ.	Max.
400 kV	80%	75	100	130	20%	75	110	150
130 kV	80%	75	110	150	20%	460	480	500
40 kV	80%	360	380	400	20%	1 840	1 860	1 880

In Section 5.4 a calculation is performed using the dip duration distribution derived in Figure 4.5 through Figure 4.7. These distributions are not based on measurements done in the calculated network, but will be used to see the differences in calculation results. The distributions are summarized in Table 5.3.

Table 5.3: Distribution of dip durations according to Figure 4.5 through Figure 4.7.

Voltage level	P _{dur. zone 1}	Min.	Typ.	Max.	P _{dur. zone 2}	Min.	Typ.	Max.
400 kV	76%	20	80	180	24%	100	250	600
130 kV	78%	100	160	320	22%	320	550	1 200
40 kV	96%	300	700	1 100	4%	1 300	1 450	1 600

5.3 Calculation using dip duration distributions from Table 5.2

The first calculation was done using fault-frequencies as shown in Table 5.1 and dip durations as shown in Table 5.2. At 130 kV the lines between busses 1309 and 1381 were shielded and also lines connected to bus 1306 were shielded the first 15 km out from bus 1306. In Figure 5.2 a scatter plot of dips due to faults from the entire calculated network during 50 years is shown. To get a comprehension of where the faults occur, 130 and 400 kV levels are calculated one at a time. The scatter plots are shown in Figure 5.3.

From the figures above the simple conclusion can be drawn that faults on 130 kV are the ones causing most problems for a customer at bus 1306. This holds both for the number of dips and their severity. To further study the source of the most severe dips faults occurring on lines directly connected to bus 1306 are separated from other faults on 130 kV. The calculation result is shown in Figure 5.4. It is obvious that the deepest dips arise from faults occurring closest to the bus. As has been noted before, shielding has been added to the lines directly connected to bus 1306 for a distance of 15 km. It has been assumed that the shielding lowers the total number of faults with 25% and also alters the proportion of different fault types (see Table 5.1!).

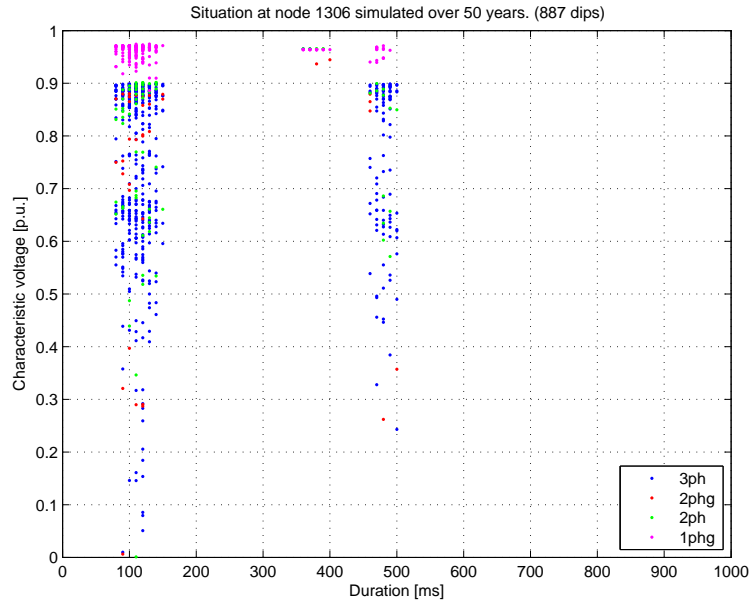


Figure 5.2: Scatter plot of the voltage dip situation at bus 1306. Faults in all voltage levels.

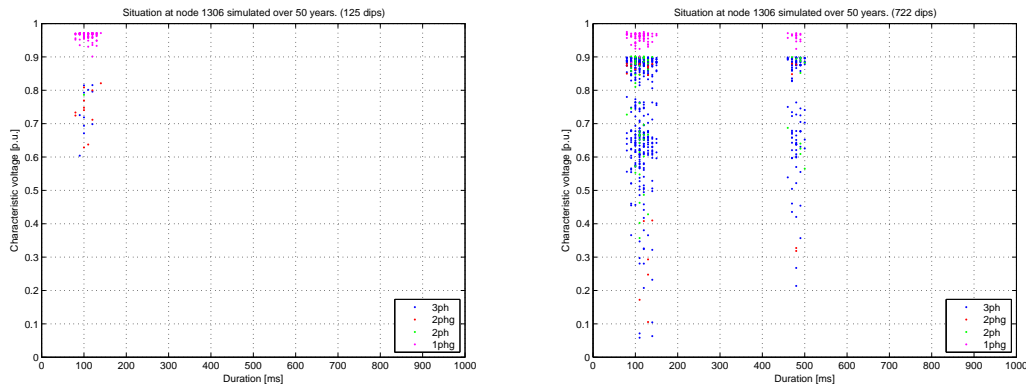


Figure 5.3: Only faults on 400 kV (left). Only faults on 130 kV (right).

To further study the dip situation the voltage dip coordination chart is presented in Figure 5.5. This coordination chart could be used together with a voltage-tolerance curve for the customer to estimate the number of production stops during a year. For example, a customer with a rectangular voltage-tolerance curve with a knee at 400 ms, 80% would experience 1.5 production stops per year. To achieve a high resolution of the chart a simulation time of 1 000 years has been used.

As a complement to the scatter plot and coordination chart the voltage dip density chart and cumulative voltage dip chart are presented in Figure 5.6 and Figure 5.7. Also here, a simulation time of 1 000 years has been used.

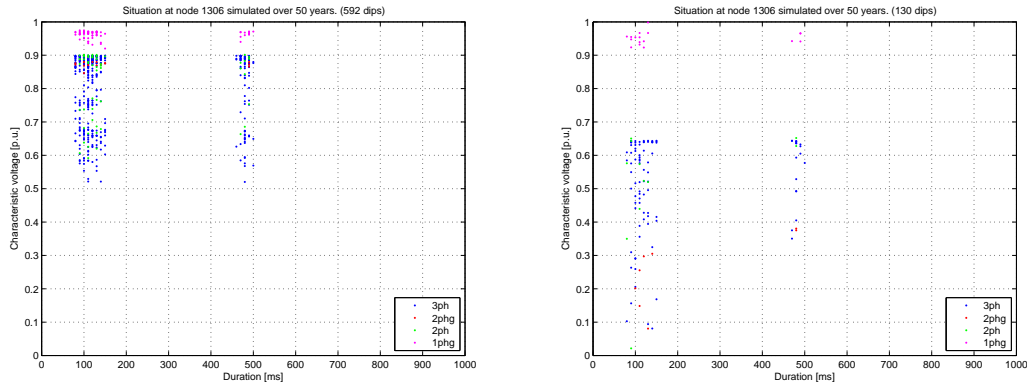


Figure 5.4: All faults on 130 kV except those on lines connected to bus 1306 (left). Only faults on lines connected to bus 1306 (right).

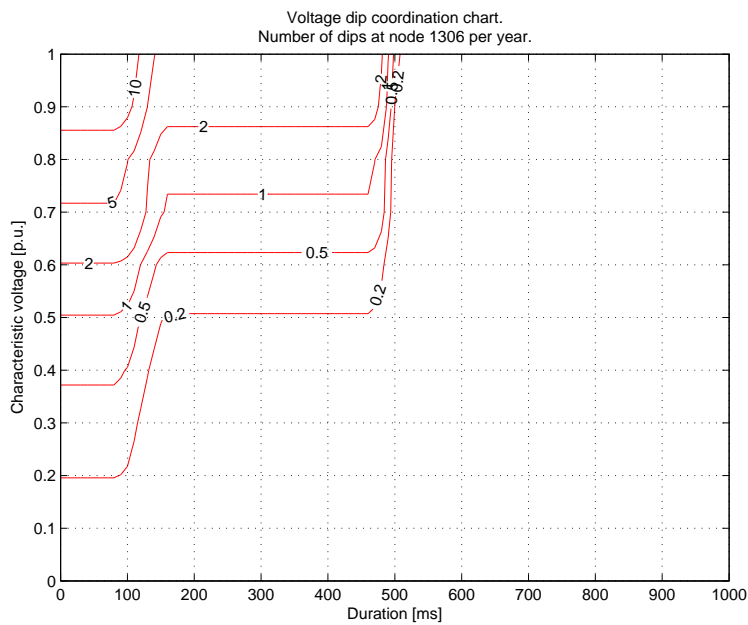


Figure 5.5: Voltage dip coordination chart of the dip situation at bus 1306.

5.3.1 Shielding added to all 130 kV lines

A possible way to lower the number of dips, and especially the number of three-phase dips, is to add shielding to all 130 kV lines. A calculation has been performed to see how this would affect the situation at bus 1306. In Figure 5.8 this improvement is compared to the dip situation for the original network by means of scatter plots and in Figure 5.9 the corresponding voltage dip coordination charts are shown. A customer with rectangular voltage-tolerance curve with a knee at 400 ms, 80% would experience 1 production stop per year (1.5 according to the original calculation). This is an improvement of 50%, but it would require extensive investments in the network.

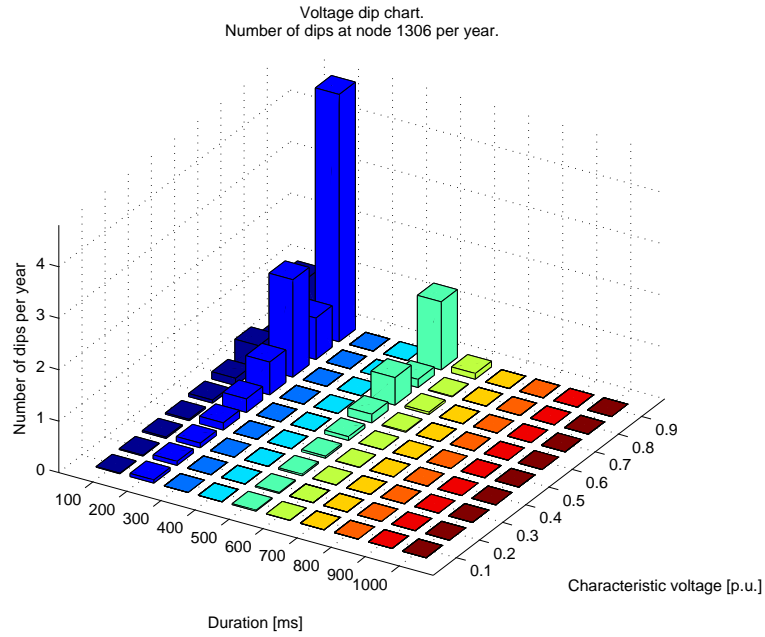


Figure 5.6: Voltage dip density chart of the dip situation at bus 1306.

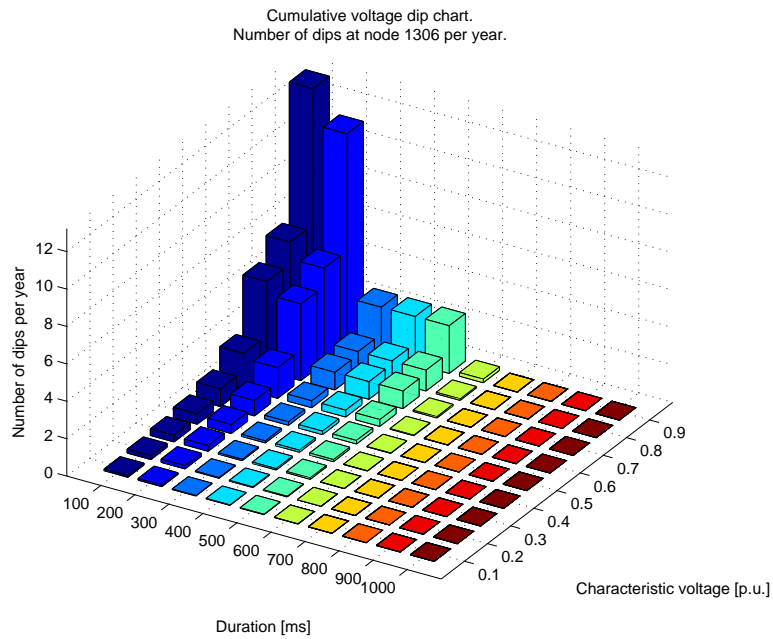


Figure 5.7: Cumulative voltage dip chart of the dip situation at bus 1306.

5.3.2 Planning of new line

To lower the vulnerability of customers connected to busses 1293 and 1306 a new line is planned between busses 1293 and 1311. A calculation is made to see how the new line is affecting customers connected to bus 1306. The new line will increase the number of faults experienced by the network but also provide an alternative way for the power delivery. The calculation re-

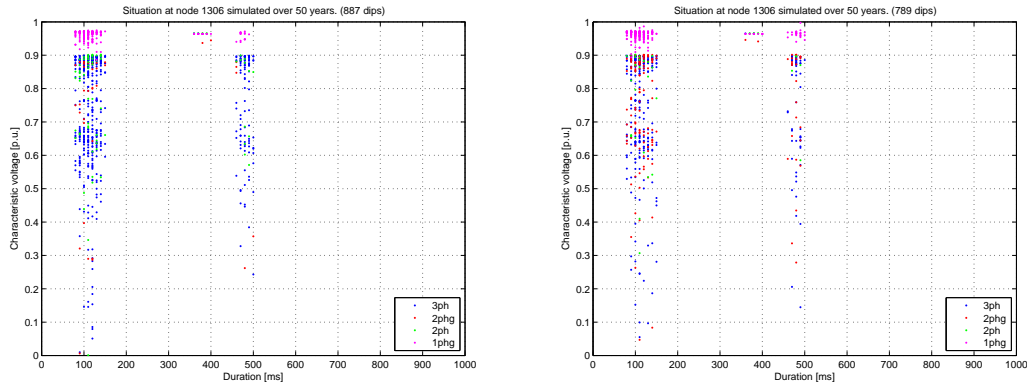


Figure 5.8: Scatter plot of dip situation. Original line setup (left) and shielding added to all 130 kV lines (right).

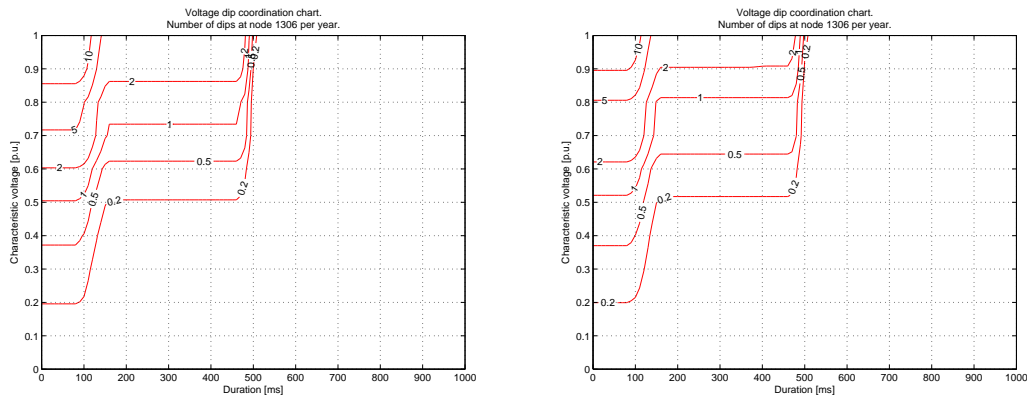


Figure 5.9: Coordination chart. Original line setup (left) and shielding added to all 130 kV lines (right).

sults are shown as scatter plot in Figure 5.10 and as coordination chart in Figure 5.11. For a customer at 1306 with a voltage-tolerance knee at 400 ms, 80%, the changes would have no significant effect.

5.3.3 Upgrading to 400 kV

The bus 1306 is connected to the transmission network via the subtransmission network. A radical change for customers connected to bus 1306 would be a direct connection to the transmission network at 400 kV. A calculation is done to study the effects on the dip situation at bus 1306 if the connection between busses 1306 and 1311 at 130 kV is replaced with a 400 kV connection between 1306 (via transformers) and 4290. The connection between 1306 and 1293 is also dropped so that bus 1306 has no direct connection to the subtransmission network. As seen from the plots in Figure 5.12 and Figure 5.13 the improvement is significant. A customer connected to bus 1306 with a voltage-tolerance knee at 400 ms, 80% would now experience 0.5 production stops a year, an improvement of over 65%. However, this upgrade would be very expensive and is not too realistic, unless there are other reasons for a direct connection to 400 kV.

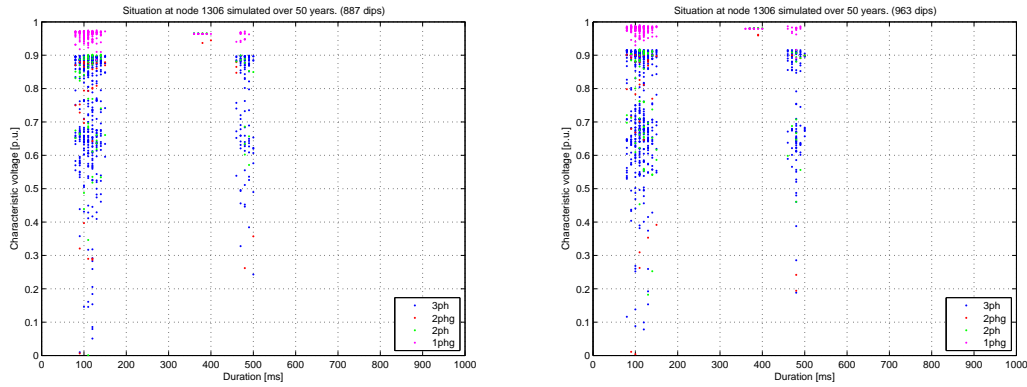


Figure 5.10: Scatter plot of dip situation. Original line setup (left) and addition of new line (right).

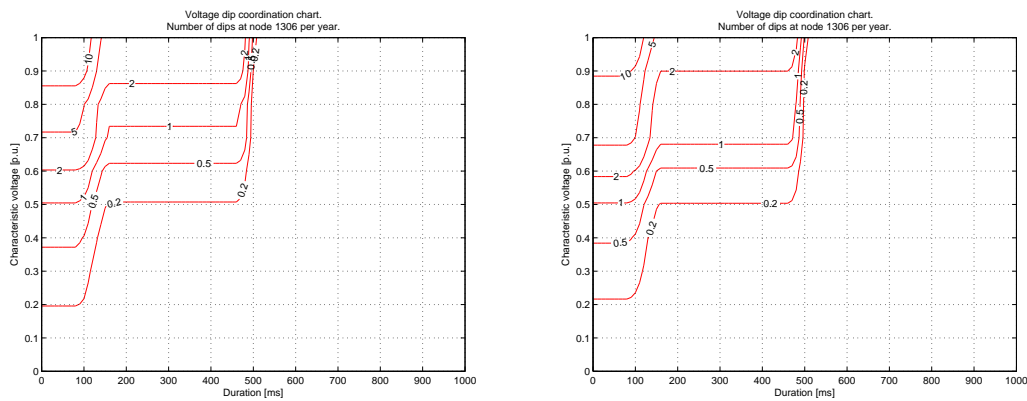


Figure 5.11: Coordination chart. Original line setup (left) and addition of new line (right).

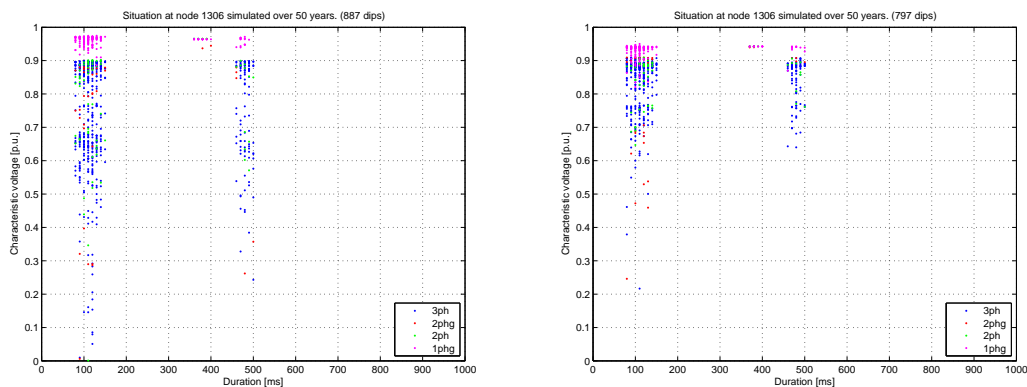


Figure 5.12: Scatter plot of dip situation. Original line setup (left) and upgrade to 400 kV (right).

5.3.4 Disconnected line during service

Consider the situation where the line between busses 1380 and 1391 is disconnected, e.g. for maintenance. The effect on the dip situation for bus 1306 is studied in a calculation. Since the

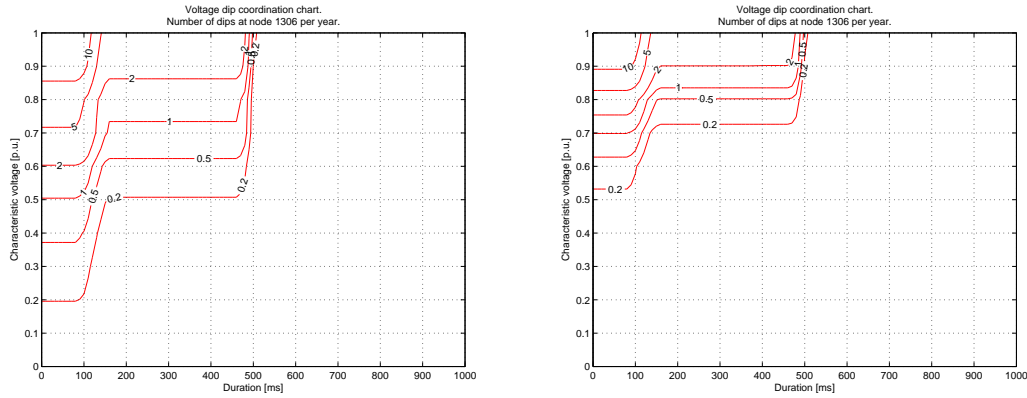


Figure 5.13: Coordination chart. Original line setup (left) and upgrade to 400 kV (right).

disconnected line makes the network vulnerable the faults result in deeper dips at bus 1306. However, this is most noticeable for dips with higher magnitude, i.e. for fault far from bus 1306. Scatter plots and coordination charts are shown in Figure 5.14 and Figure 5.15. A customer connected to bus 1306 with a voltage-tolerance knee at 400 ms, 80% would experience 1.75 production stops a year during the service, an increase of 16%. This may appear a small increase, but as many dips occur due to lightning, it could be decided to avoid maintenance during seasons with high lightning frequency.

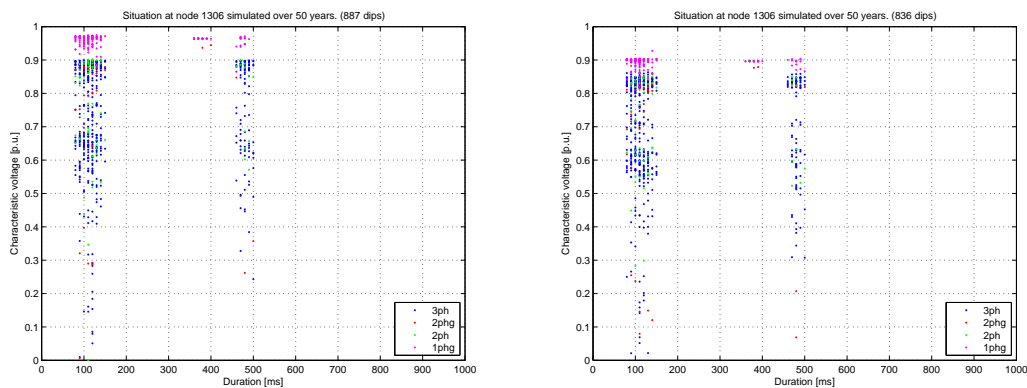


Figure 5.14: Scatter plot of dip situation. Original line setup (left) and with line disconnected (right).

5.4 Calculation using dip duration distributions from Table 5.3

In the calculation presented here, the dip duration distributions are taken from Table 5.3. The measurements used to obtain these distributions were not made in the network being calculated on, but they still give a realistic view of how dips could be distributed along the duration axis. In Figure 5.16 the scatter plot is presented for a simulation over 50 years.

In Figure 5.17 the coordination chart is given for the dip situation at bus 1306. The simulation is done over 1 000 years. Voltage dip density chart and cumulative voltage dip chart are

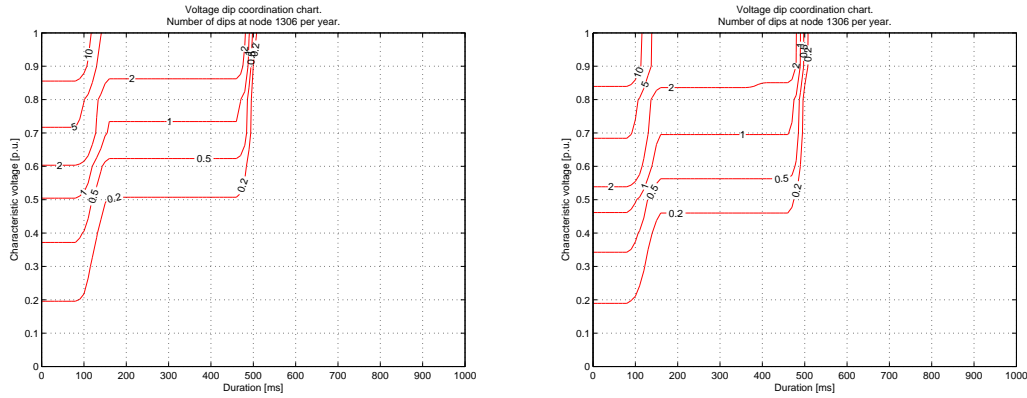


Figure 5.15: Coordination chart. Original line setup (left) and with line disconnected (right).

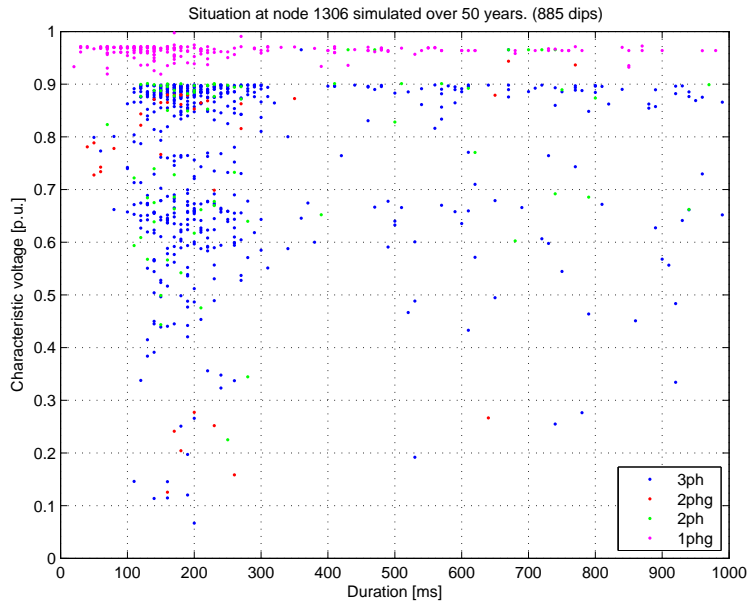


Figure 5.16: Scatter plot of the dip situation at bus 1306.

presented in Figure 5.18 and Figure 5.19. A customer connected to bus 1306, using equipment with a voltage-tolerance knee at 400 ms, 80%, would still experience about 1.5 trips per year. This can be seen as a coincidence, since there are significant differences between Figure 5.16 and Figure 5.5.

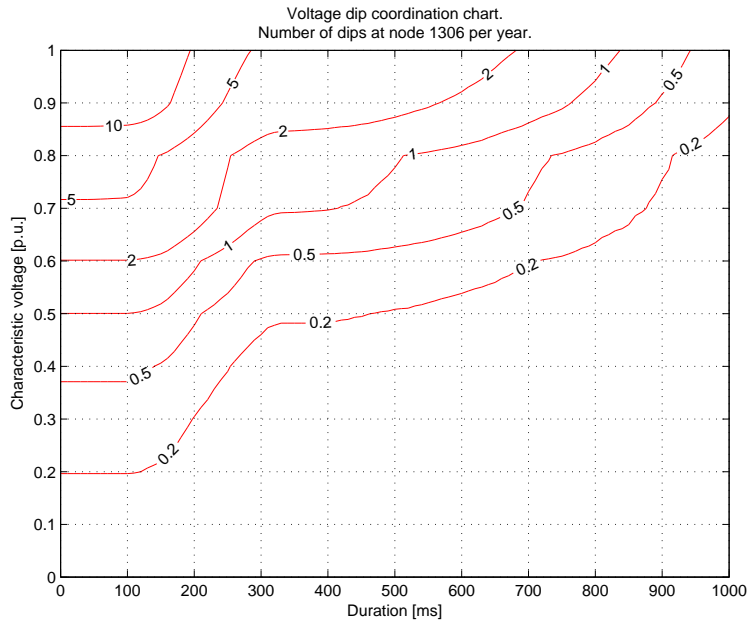


Figure 5.17: Voltage dip coordination chart of the dip situation at bus 1306.

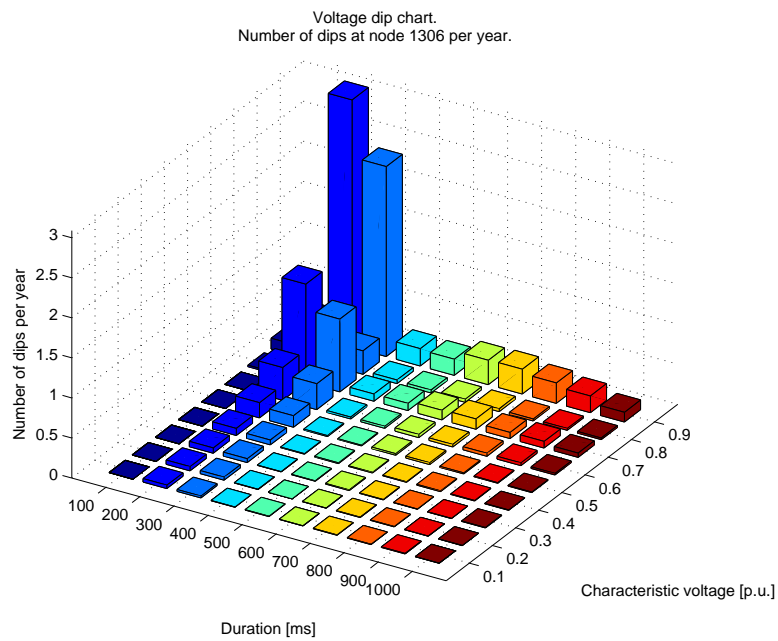


Figure 5.18: Voltage dip density chart of the dip situation at bus 1306.

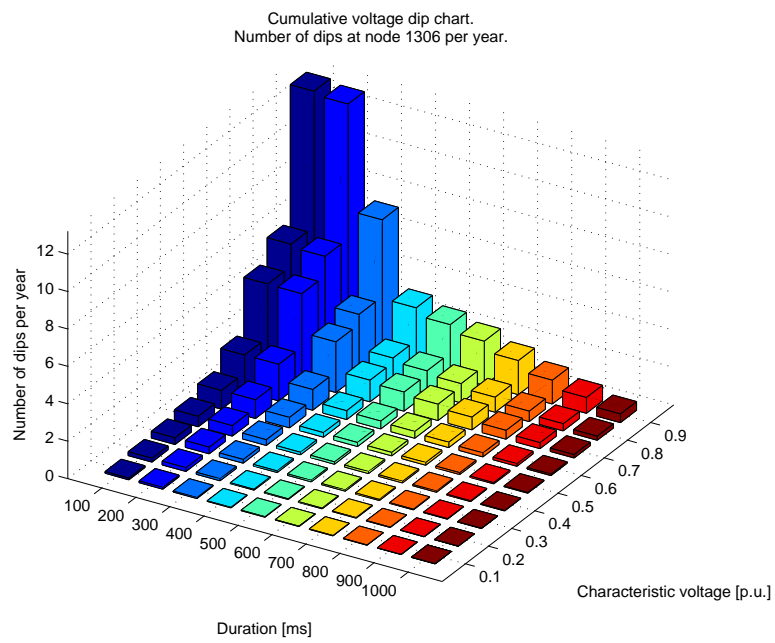


Figure 5.19: Cumulative voltage dip chart of the dip situation at bus 1306.

6 Discussion

In this report three parts of the voltage dip calculation have been treated: the dip duration, the dip magnitude and the graphical presentation of the calculation results. These parts will be discussed in the following three sections.

6.1 Calculation of dip duration

It was shown in Section 4.1 that even with an extensive knowledge of the network and of the protection systems used in the network it is difficult—if not impossible—to determine an exact dip duration for a fault somewhere in the network. A method for defining statistical distributions of dip durations for subsets of the network was introduced. The subsets are chosen according to voltage level in the network, since in general similar distributions hold for dips originating at one voltage level. The method is able to produce calculation results with good accuracy under an important condition: that the data used as basis for the distributions is of sufficient accuracy. This data can be collected in different ways, but monitoring the network (or a network with similar characteristics) together with knowledge of the protection relay settings can give data of desired accuracy.

Only calculation of voltage dips as result of faults in the network are considered here and it should be noted that voltage dips could occur for other reasons too. All events that cause a large current to flow in some part of the network can result in voltage dips at exposed locations in the network. Starting of large machines and energizing of large transformers are two examples. For an environment with, e.g., many large induction motors this needs to be taken into consideration, but in general the majority of the more severe dips are the result of faults. Thus, concentrating on dips due to faults is an acceptable simplification.

In general, fault-frequencies for the different fault types (three-phase, two-phase-to-ground, phase-to-phase and single-phase-to-ground) are not easily accessed. Recorded faults in statistical reports are often identified with their cause rather than divided into fault types. However, it is shown in [13] how probabilities for different fault types can be derived from the pole configuration. This information can be used to form a basis for the fault-frequencies.

6.2 Calculation of dip magnitude

Most faults in a power system occur on overhead lines and equations can be found in literature for calculating the resulting dip magnitude (or characteristic voltage) at a certain node in the network, a method called the Moving Fault Node. In the existing version of Simpov Dips the dip magnitudes are calculated with faults only occurring at the nodes. Since every line has an impedance that affects the dip magnitude the implementation of the Moving Fault Node method will result in more accurate calculations of the magnitude.

The calculation requires the bus impedance matrix, the impedance for the faulted line, the fault position on the line and pre-fault voltages at three places in the system: the two terminals

of the faulted line and the node where the customer is connected. All these parameters, except the fault position, are available in Simpow Dips and thus an implementation of this method did not require additional network information to be added. The fault position on the line, λ , is assumed to be a stochastic variable with a uniform distribution over the line length.

The assumption of a uniformly distributed λ can be argued about. Of course different types of distribution could be used for different lines (e.g. convex or concave) and the fault-frequency along a long line could vary substantially depending on its environment. A more practical approach than defining complicated distributions to the line is to divide it into shorter sections, each with its own fault-frequency. In reality this method is more accurate. Consider a line that is partially shielded. The shielded part will experience fewer faults than the unshielded, but more important, the proportion of fault types (three-phase, two-phase-to-ground, phase-to-phase and single-phase-to-ground) will vary significantly [13]. Only altering the distribution of λ will not take this difference into account. By inserting a fictitious node along the line, two lines with completely different fault-frequencies can be defined.

In Section 4.2 it is shown how the Moving Fault Node method can be extended to calculate the characteristic voltage for unbalanced dips. These calculations require the bus impedance matrix for positive, negative and zero sequence and also the sequence impedances for the faulted line. The calculation of the dip magnitude for a fault at a line is not yet implemented in Simpow Dips, but is done in an analysis Matlab program that also produces the graphical plots. The result-file produced by Simpow Dips gives pre-fault voltages and sequence impedances necessary for the calculation.

6.3 Graphical presentation of calculation results

To get a good picture of the voltage dip situation different graphical presentations of the calculated dips can be produced. In the Matlab analysis program scatter plots, voltage dip coordination charts and voltage dip density charts are produced. The voltage dip coordination chart is helpful when estimating the severity of the dip situation for a certain customer by introducing the voltage-tolerance curve. By using the voltage dip density chart and cumulative chart a picture of the power quality is given for the site.

The different plots also simplify the analysis of the effect of changes in the power system. This was shown in Chapter 5 for a number of different changes to a small network.

When creating the different plots one need to consider the number of years to simulate over. This depends on the type of plot and also on the different fault-frequencies of the components in the network. Different simulation times can be needed for different kind of plots. For a scatter plot, around 1 000 events will give an informative picture of the situation. In general a simulation over a few hundred years is sufficient, but this may result in a very clogged scatter plot in case of high fault-frequencies. To create reliable coordination and voltage dip density charts, a longer simulation time is often needed.

The Matlab analysis program limits the simulation to 1 second even though the definition of voltage dips gives a duration of 0.5 cycle to 1 minute. This narrow time window can be argued for since deep dips longer than 1 second are unusual and point to some serious problem in the network. Also, an increase of the customer's immunity to dip durations longer than 1 second will probably be very costly.

7 Future work

The calculation model of dip durations using statistical distributions needs to be validated by comparing calculations with measurements made in the same network. To further increase the applicability of the calculation software an additional duration zone could be implemented (giving a total of three duration zones). Instead of the current result-file (or as a complement to it), a matrix containing all calculated dips with relevant data could be created by the software. This would need much of the code now made in Matlab to be implemented in Simpov Dips. The following data could be contained in the matrix for each dip event: duration, characteristic voltage, PN factor, fault location causing the dip, dip type (A, B, C or D). With this information the desired plots and analysis can be made in a software chosen by the user.

References

- [1] Bollen, M.H.J., Understanding power quality problems: voltage sags and interruptions, 2000, online material at [ftp.ieee.org/uploads/press/Bollen](ftp://ftp.ieee.org/uploads/press/Bollen).
- [2] IEEE Std. 1159-1995, IEEE Recommended Practice for Monitoring Electric Power Quality.
- [3] Bollen, M.H.J. and Zhang, L.D., A method for characterization of three-phase unbalanced dips from recorded voltage waveshapes, lecture notes from Chalmers University of Technology.
- [4] Bollen, M.H.J., *Understanding power quality problems: voltage sags and interruptions*, New York: IEEE, Inc., 2000.
- [5] Bollen, M.H.J. and Zhang, L.D., Different methods for classification of three-phase unbalanced voltage dips due to faults, *Electric Power Systems Research* 66, pp. 59–69, 2003.
- [6] Demcko, J.A. and Sullivan, S., Power quality problems and solutions at Arizona public service company, *7th IEEE Int. Conf. on Harmonics and Quality of Power (ICHQP)*, pp. 348–353, October 1996.
- [7] IEEE Std. 1346-1998, IEEE Recommended Practice for Evaluating Electric Power System Compability With Electronic Process Equipment.
- [8] Utveckling Elkvalitet, Slutrapport, Elforsk rapport 04:46, 2004.
- [9] Olguin, G., *Voltage Dip (Sag) Estimation in Power Systems based on Stochastic Assessment and Optimal Monitoring*, Ph.D. thesis, Chalmers University of Technology, Göteborg, 2005.
- [10] Bollen, M.H.J. and Gu, I.Y.H., *Signal processing of power quality disturbances*, New York: Wiley-IEEE Press, 2006.
- [11] Lim, Y.S., *Probabilistic Assessments of Voltage-Sag Occurrence and the Evaluation of the Dynamic Voltage Restorer Capability*, Ph.D. thesis, University of Manchester.
- [12] Kenjar, I. and Olsson, M., *Voltage dips: voltage dip characteristics of a bus due to faults in the surrounding network*, Master's thesis, Chalmers University of Technology, Göteborg, 2003.
- [13] Karlsson, D., Norberg, P. and Bollen, M.H.J., Different Fault Types and Voltage Dips in relation to Shielding of Subtransmission Lines, submitted to IEEE Transactions on Power Delivery.
- [14] Heine, P. and Lehtonen, M., Voltage Sag Distribution Caused by Power System Faults, *IEEE Transactions on Power Systems*, volume 18(4), November 2003.

A Simpow files used in calculation

Simpow Dips uses three different files: an otnes file produced from a Simpow optpow calculation, a dynpow file containing dynamic information of the network and a fault-information file described in the report. During the calculations presented in Chapter 5 a simple network was used. In this appendix the input files are presented.

A.1 Optpow file

ÖVNINGSNÄT 400 - 130 KV

**

CONTROL DATA

UBCHECK=NO

NSEP=NO

END

GENERAL

SN=1000.000

END

NODES

1293 UB=135.000

1293A UB=135.000

1294 UB=135.000

1296 UB=135.000

1300 UB=135.000

1305 UB=135.000

1306 UB=135.000

1306A UB=135.000

1309 UB=135.000

1311 UB=135.000

1318 UB=135.000

1380 UB=135.000

1381 UB=135.000

1383 UB=135.000

1391 UB=135.000

1399 UB=135.000

4250 UB=400.000

4290 UB=400.000

4380 UB=400.000

7001 UB=400.000

7002 UB=400.000

A UB=135.000

B UB=40.000

C UB=40.000

END

SREACTORS

1296 1309 TYPE=11 R=0.147550 X=0.827480

END

LINES

1293 1296 NO=1 TYPE=12 R=0.387117E-02 X=0.213417E-01 B=0.546012E-04 L=16.30
 1293 1305 NO=1 TYPE=12 R=0.374562E-02 X=0.208592E-01 B=0.534743E-04 L=33.10
 1306 A NO=1 TYPE=12 R=0.219639E-02 X=0.206145E-01 B=0.534137E-04 L=3.50
 A 1293A NO=1 TYPE=12 R=0.219639E-02 X=0.206145E-01 B=0.534137E-04 L=11.50
 1293A 1293 NO=1 TYPE=12 R=0.219639E-02 X=0.206145E-01 B=0.534137E-04 L=9.50
 B C NO=1 TYPE=12 R=0.219639E-02 X=0.206145E-01 B=0.534137E-04 L=11.50
 B C NO=2 TYPE=12 R=0.219639E-02 X=0.206145E-01 B=0.534137E-04 L=11.50
 1294 1300 NO=1 TYPE=12 R=0.365799E-02 X=0.208454E-01 B=0.497717E-04 L=43.80
 1294 1311 NO=1 TYPE=12 R=0.368429E-02 X=0.209286E-01 B=0.500000E-04 L=7.00
 1294 1318 NO=1 TYPE=12 R=0.385357E-02 X=0.212940E-01 B=0.547619E-04 L=8.40
 1300 1383 NO=1 TYPE=12 R=0.365791E-02 X=0.208575E-01 B=0.497863E-04 L=46.80
 1305 1311 NO=1 TYPE=12 R=0.222083E-02 X=0.205435E-01 B=0.535714E-04 L=16.80
 1305 1311 NO=2 TYPE=12 R=0.227836E-02 X=0.205363E-01 B=0.543860E-04 L=17.10
 1306 1306A NO=1 TYPE=12 R=0.224277E-02 X=0.205701E-01 B=0.534307E-04 L=15.00
 1306A 1311 NO=1 TYPE=12 R=0.224277E-02 X=0.205701E-01 B=0.534307E-04 L=15.00
 1309 1399 NO=1 TYPE=12 R=0.278244E-02 X=0.208590E-01 B=0.336585E-04 L=41.00
 1311 1318 NO=1 TYPE=12 R=0.306087E-02 X=0.207957E-01 B=0.760870E-04 L=18.40
 1380 1391 NO=1 TYPE=12 R=0.209942E-02 X=0.205959E-01 B=0.536232E-04 L=34.50
 1381 1383 NO=1 TYPE=12 R=0.365141E-02 X=0.208271E-01 B=0.496479E-04 L=28.40
 1381 1399 NO=1 TYPE=12 R=0.277671E-02 X=0.208241E-01 B=0.578313E-04 L=24.90
 1383 1391 NO=1 TYPE=12 R=0.367122E-02 X=0.208820E-01 B=0.496403E-04 L=13.90
 4250 4290 NO=1 TYPE=12 R=0.166609E-03 X=0.200052E-02 B=0.538408E-03 L=57.80
 4250 4380 NO=1 TYPE=12 R=0.116016E-03 X=0.175048E-02 B=0.647991E-03 L=176.70
 4290 4380 NO=1 TYPE=12 R=0.166667E-03 X=0.200000E-02 B=0.541667E-03 L=120.00
 4290 7001 NO=1 TYPE=12 R=0.116352E-03 X=0.175067E-02 B=0.645103E-03 L=111.30
 4380 7002 NO=1 TYPE=12 R=0.178180E-03 X=0.199981E-02 B=0.541318E-03 L=107.70
 7001 7002 NO=1 TYPE=12 R=0.115017E-03 X=0.175119E-02 B=0.602048E-03 L=29.30
 1380 1381 NO=1 TYPE=12 R=0.277731E-02 X=0.208640E-01 B=0.578704E-04 L=64.80

END

TRANSFORMERS

1311 4290 NO=1 SN=1000.000 UN1=135.000 UN2=400.000 ER12=0.00100 EX12=0.16000 FI=0.00
 TAPSIDE=1 STEP=0.16700E-01 +NSTEP=8 -NSTEP=8
 1311 4290 NO=2 SN=1000.000 UN1=135.000 UN2=400.000 ER12=0.00180 EX12=0.20000 FI=0.00
 TAPSIDE=1 STEP=0.16700E-01 +NSTEP=8 -NSTEP=8
 1380 4380 NO=1 SN=1000.000 UN1=135.000 UN2=400.000 ER12=0.00300 EX12=0.19000 FI=0.00
 TAPSIDE=1 STEP=0.82653E-02 +NSTEP=16 -NSTEP=4
 1380 4380 NO=2 SN=1000.000 UN1=135.000 UN2=400.000 ER12=0.00300 EX12=0.19000 FI=0.00
 TAPSIDE=1 STEP=0.82653E-02 +NSTEP=16 -NSTEP=4
 B A NO=1 SN=63.000 UN1=40.000 UN2=135.000 ER12=0.00000 EX12=2.79756 FI=0.00
 TAPSIDE=1

END

SHUNT IMPEDANCES

1293 P=0.000 Q=-37.000 UN=135.000
 1305 P=0.000 Q=-35.000 UN=135.000
 1311 P=0.000 Q=-90.000 UN=135.000
 1318 P=0.000 Q=-60.000 UN=135.000

END

LOADS

1293 NO=1 P=30.000 Q=0.000 MP=1 MQ=1
 1296 NO=1 P=7.000 Q=0.000 MP=1 MQ=1
 1300 NO=1 P=10.500 Q=0.000 MP=1 MQ=1
 1305 NO=1 P=30.000 Q=0.000 MP=1 MQ=1
 1306 NO=1 P=15.000 Q=0.000 MP=1 MQ=1
 1309 NO=1 P=11.000 Q=0.000 MP=1 MQ=1
 1311 NO=1 P=75.000 Q=0.000 MP=1 MQ=1
 1318 NO=1 P=70.000 Q=0.000 MP=1 MQ=1
 1380 NO=1 P=45.000 Q=0.000 MP=1 MQ=1
 1381 NO=1 P=10.000 Q=0.000 MP=1 MQ=1
 1391 NO=1 P=34.000 Q=0.000 MP=1 MQ=1
 1399 NO=1 P=5.000 Q=0.000 MP=1 MQ=1

```

4250 NO=1 P=100.000 Q=0.000 MP=1 MQ=1
7001 NO=1 P=30.000 Q=0.000 MP=1 MQ=1
1293 NO=2 P=1.000 Q=90.000 MP=0 MQ=0
1296 NO=2 P=1.000 Q=30.000 MP=0 MQ=0
1300 NO=2 P=1.000 Q=67.500 MP=0 MQ=0
1305 NO=2 P=1.000 Q=123.000 MP=0 MQ=0
1306 NO=2 P=1.000 Q=60.000 MP=0 MQ=0
1309 NO=2 P=1.000 Q=35.000 MP=0 MQ=0
1311 NO=2 P=1.000 Q=278.000 MP=0 MQ=0
1318 NO=2 P=1.000 Q=220.000 MP=0 MQ=0
1380 NO=2 P=1.000 Q=300.000 MP=0 MQ=0
1381 NO=2 P=1.000 Q=51.000 MP=0 MQ=0
1391 NO=2 P=1.000 Q=88.000 MP=0 MQ=0
1399 NO=2 P=1.000 Q=19.000 MP=0 MQ=0
4250 NO=2 P=1.000 Q=800.000 MP=0 MQ=0
7001 NO=2 P=1.000 Q=150.000 MP=0 MQ=0
END
POWER CONTROL
4380 TYPE=NODE NAME=V_GG1 RTYP=SW U=408.000000 FI=-13.6758
1306 TYPE=NODE NAME=L_GG1 RTYP=UP U=143.0001 P=175.000 QMIN=0.000000 QMAX=80.00000
1306 TYPE=NODE NAME=L_GG2 RTYP=UP U=143.0001 P=175.000 QMIN=0.000000 QMAX=80.00000
4250 TYPE=NODE NAME=G_GG1 RTYP=UP U=405.0000 P=150.000 QMIN=-200.0000 QMAX=200.0000
7002 TYPE=NODE NAME=N_GG1 RTYP=UP U=408.0000 P=800.000 QMIN=-200.0000 QMAX=300.0000
1311 4290 NO=1 TYPE=TREG RTYP=UFI TAU=1.03340 FI=0.000 CNODE=1311 U=135.00000
1311 4290 NO=2 TYPE=TREG RTYP=UFI TAU=1.03340 FI=0.000 CNODE=1311 U=135.00000
1380 4380 NO=1 TYPE=TREG RTYP=UFI TAU=1.03304 FI=0.000 CNODE=1380 U=135.00000
1380 4380 NO=2 TYPE=TREG RTYP=UFI TAU=1.03304 FI=0.000 CNODE=1380 U=135.00000
END
END

```

A.2 Dynpow file

ÖVNINGSNÄT 400 - 130 KV

```

-----
**
CONTROL DATA
  UBCHECK=NO
  NSEP=NO
END
GENERAL DATA
  FN=50.000
  REF=V_GG1
END
LINES
1293 1296 NO=1 R0=0.26502 X0=0.93925 B0=0.00134
1293 1305 NO=1 R0=0.52072 X0=1.86419 B0=0.00265
1306 A    NO=1 R0=0.22970 X0=1.38591 B0=0.00200
A      1293A NO=1 R0=0.22970 X0=1.38591 B0=0.00200
1293A 1293 NO=1 R0=0.22970 X0=1.38591 B0=0.00200
B      C    NO=1 R0=0.22970 X0=1.38591 B0=0.00200
B      C    NO=2 R0=0.22970 X0=1.38591 B0=0.00200
1294 1300 NO=1 R0=0.67292 X0=2.46518 B0=0.00327
1294 1311 NO=1 R0=0.10832 X0=0.39555 B0=0.00052
1294 1318 NO=1 R0=0.13595 X0=0.48295 B0=0.00069
1300 1383 NO=1 R0=0.71900 X0=2.63555 B0=0.00350
1305 1311 NO=1 R0=0.15670 X0=0.93185 B0=0.00135
1305 1311 NO=2 R0=0.16363 X0=0.94816 B0=0.00140
1306 1306A NO=1 R0=0.64525 X0=3.80444 B0=0.00549
1306A 1311 NO=1 R0=0.64525 X0=3.80444 B0=0.00549
1309 1399 NO=1 R0=0.47914 X0=2.30909 B0=0.00207

```

1311 1318 NO=1 R0=0.23654 X0=1.03313 B0=0.00210
 1380 1381 NO=1 R0=0.75587 X0=3.65037 B0=0.00563
 1380 1391 NO=1 R0=0.30421 X0=1.91851 B0=0.00277
 1381 1383 NO=1 R0=0.43554 X0=1.59702 B0=0.00212
 1381 1399 NO=1 R0=0.29039 X0=1.40000 B0=0.00216
 1383 1391 NO=1 R0=0.21433 X0=0.78370 B0=0.00104
 4250 4290 NO=1 R0=0.04045 X0=0.31220 B0=0.04668
 4250 4380 NO=1 R0=0.08610 X0=0.83514 B0=0.17175
 4290 4380 NO=1 R0=0.08400 X0=0.64800 B0=0.09750
 4290 7001 NO=1 R0=0.05439 X0=0.52609 B0=0.10770
 4380 7002 NO=1 R0=0.08060 X0=0.58153 B0=0.08745
 7001 7002 NO=1 R0=0.01415 X0=0.13854 B0=0.02646

END

TRANSFORMERS

1311 4290 NO=1 CP1=Y CP2=Y EX120=0.24000
 1311 4290 NO=2 CP1=Y CP2=Y EX120=0.20000
 1380 4380 NO=1 CP1=Y CP2=Y EX120=0.19000
 1380 4380 NO=2 CP1=Y CP2=Y EX120=0.19000
 B A NO=1 CP1=D CP2=D EX120=2.79756

END

SYNCHRONOUS MACHINES

L_GG1 1306 TYPE=4 XD=0.750000 SN=200.00 UN=135.0000 XQ=0.250000 XDP=0.250000 RA=0.00000 H=9999
 L_GG2 1306 TYPE=4 XD=0.750000 SN=200.00 UN=135.0000 XQ=0.250000 XDP=0.250000 RA=0.00000 H=9999
 G_GG1 4250 TYPE=4 XD=0.710000 SN=950.00 UN=400.0000 XQ=0.210000 XDP=0.210000 RA=0.00000 H=9999
 V_GG1 4380 TYPE=4 XD=0.720000 SN=1500.00 UN=400.0000 XQ=0.220000 XDP=0.220000 RA=0.00000 H=9999
 N_GG1 7002 TYPE=4 XD=0.720000 SN=1000.00 UN=400.0000 XQ=0.220000 XDP=0.220000 RA=0.00000 H=9999

END

SREACTORS

1296 1309 R0=0.61971 X0=2.23420

END

END

A.3 Fault-information file

NODE

1293 0 0 0 0
 1293A 0 0 0 0
 1294 0 0 0 0
 1296 0 0 0 0
 1300 0 0 0 0
 1305 0 0 0 0
 1306 0 0 0 0
 1306A 0 0 0 0
 1309 0 0 0 0
 1311 0 0 0 0
 1318 0 0 0 0
 1380 0 0 0 0
 1381 0 0 0 0
 1383 0 0 0 0
 1391 0 0 0 0
 1399 0 0 0 0
 4250 0 0 0 0
 4290 0 0 0 0
 4380 0 0 0 0
 7001 0 0 0 0
 7002 0 0 0 0
 A 0 0 0 0
 B 0 0 0 0
 C 0 0 0 0

END

SIMPOW FILES USED IN CALCULATION

LINES

B C 1 0.00249 0.00142 0.00819 0.02350
B C 2 0.00249 0.00142 0.00819 0.02350
1293 1296 1 0.02400 0.00000 0.00300 0.00300
1293 1305 1 0.02400 0.00000 0.00300 0.00300
1306 A 1 0.01325 0.00550 0.00125 0.00500
A 1293A 1 0.01325 0.00550 0.00125 0.00500
1293A 1293 1 0.02400 0.00000 0.00300 0.00300
1294 1300 1 0.02400 0.00000 0.00300 0.00300
1294 1311 1 0.02400 0.00000 0.00300 0.00300
1294 1318 1 0.02400 0.00000 0.00300 0.00300
1300 1383 1 0.02400 0.00000 0.00300 0.00300
1305 1311 1 0.02400 0.00000 0.00300 0.00300
1305 1311 2 0.02400 0.00000 0.00300 0.00300
1306 1306A 1 0.01325 0.00550 0.00125 0.00500
1306A 1311 1 0.02400 0.00000 0.00300 0.00300
1309 1399 1 0.01325 0.00550 0.00125 0.00500
1311 1318 1 0.02400 0.00000 0.00300 0.00300
1380 1391 1 0.02400 0.00000 0.00300 0.00300
1380 1381 1 0.02400 0.00000 0.00300 0.00300
1381 1383 1 0.02400 0.00000 0.00300 0.00300
1381 1399 1 0.01325 0.00550 0.00125 0.00500
1383 1391 1 0.02400 0.00000 0.00300 0.00300
4250 4290 1 0.00040 0.00036 0.00008 0.00336
4250 4380 1 0.00040 0.00036 0.00008 0.00336
4290 4380 1 0.00040 0.00036 0.00008 0.00336
4290 7001 1 0.00040 0.00036 0.00008 0.00336
4380 7002 1 0.00040 0.00036 0.00008 0.00336
7001 7002 1 0.00040 0.00036 0.00008 0.00336

END

DURATION

40 0.8 360 380 400 0.2 1840 1860 1880
135 0.8 75 110 150 0.2 460 480 500
400 0.8 75 100 130 0.2 75 110 150

END